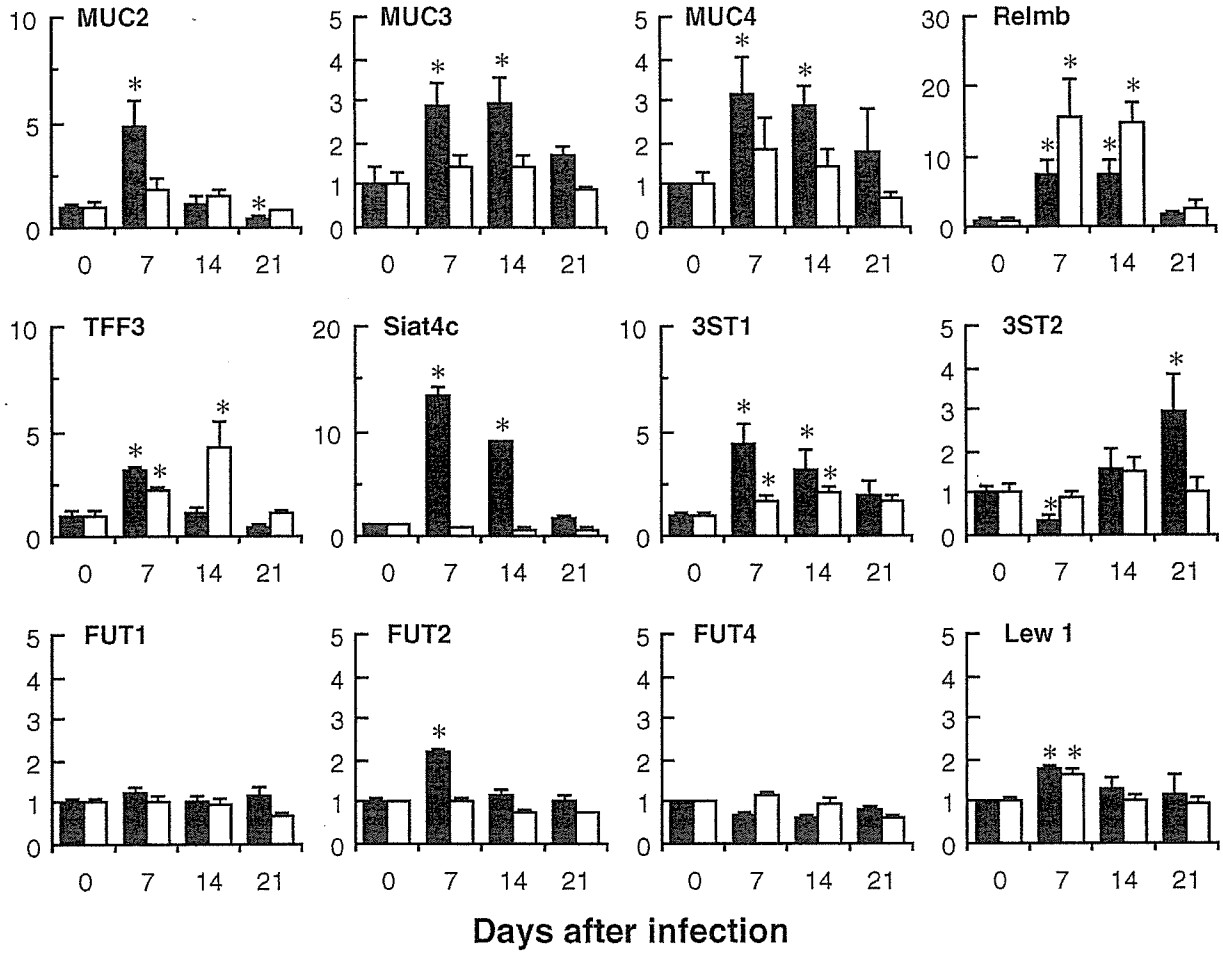

Fig 1. Expression of goblet cell- and mucin glycosylation-related genes in the jejunal (closed columns) and ileal (open columns) villus epithelium of BN rats after infection with the nematode *N. brasiliensis.* Total RNA was extracted from the epithelial fraction, reverse transcribed, and relative quantification was carried out by RT-PCR. The quantified value for each sample was normalized with respect to that for β-action. The data are means+SE of four animals. The vertical axis shows the expression levels, with day-0 average levels expressed as 1.0. *Indicates values significantly different from the day-0 level ($p<0.05$).

expression were observed after nematode infection (data not shown). It has been reported that MUC2 and MUC3 mRNA expression was increased in the small intestinal epithelium after infection with the epithelium-invading nematode *T. spiralis* in mice (31). The present findings that not only MUC2 and MUC3, but also MUC4 mRNA expression was upregulated after infection suggest that the mucin response to nematode infection might have occurred not only in goblet cells, but also in columnar cells.

The gene expression of goblet cell-specific non-mucin peptide Relmβ, whose expression is dependent on Th2 cytokines and has a potentially important role in protective immunity (11, 17), was also upregulated after infection (Fig. 1), consistent with previous reports showing that Relmβ expression was induced after infection of mice with *Trichuris muris, T. spiralis and N. brasiliensis* (11, 17). The finding that strong upregulation of Relmβ occurred not only in the jejunum, but also in the ileum, where scarcely any parasites were found, may reflect the systemic effect of Th2 cytokines. TFF3, which might protect mucous epithelia from a range of insults and is known to contribute to mucosal repair (18, 19), was also upregulated, consistent with its upregulation in *T. spiralis*-infected mice (32). In a previous report, TFF3 gene expression was not altered in mice infected with *N. brasiliensis* (33); the discrepancy may possibly be due to the difference of host species.

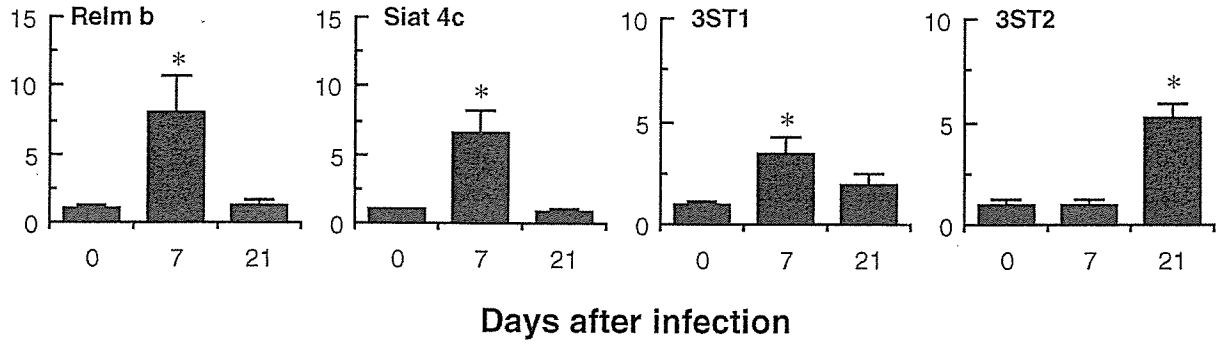

Fig. 2. Expression of mucin glycosylation-related genes in the jejunal villus epithelium of mast cell-deficient *Ws/Ws* rats after infection with the nematode *N. brasiliensis*. Total RNA was extracted from the epithelial fraction and semi-quantitative RT-PCR was performed as described in Fig. 1. The data are means+SE of four animals. The vertical axis shows the expression levels, with day-0 average levels expressed as 1.0. *Indicates values significantly different from the day-0 level ($p<0.05$).

Not only the production and secretion of mucins and goblet cell-specific peptides, but also the glycosylation status of the terminal sugar chains of mucins and/or membrane glycoproteins might have an important role in the colonization of nematodes in and/or rejection of nematodes from the intestine. Although a variety of glycosyltransferases may be involved in the modulation of the terminal sugar chains of mucins and membrane glycoproteins, little is known about the dynamic changes of these genes after infection, except that the upregulation of Siat 4c, FUT2 or A-type transferase has been reported in mice or rats after infection with *T. spiralis* or *N. brasiliensis* (9–11). The present results showed that the gene expression of Siat 4c, 3ST1, 3ST2, FUT2 and Lewl was upregulated after infection (Fig. 1), showing for the first time that not only sialyltransferase and fucosyltransferase but also sulfotransferase gene expression changed during nematode infection. The slight upregulation of the FUT2 and Lewl genes after infection suggests that some changes also occurred in the histo-blood antigens after infection. Although the upregulation of these genes was transient and the levels of the mRNAs returned to steady state levels by 21 days PI, 3ST2 expression was instead upregulated 21 days PI, suggesting that the expression of the two sulfotransferases is regulated by different mechanisms.

Several types of glycosylation-related genes, especially O-sulfotransferase genes, are considered to be specifically expressed in mast cells, which synthesize sulfated glycosaminoglycans such as heparin and/or chondroitin sulfate (34). It is well established that the number of mast cells increases not only in the propria mucosa, but also in the epithelium, after *N. brasiliensis* infection (35). Thus, intraepithelial mast cells contaminating the epithelial fraction might be responsible for the upregulation of 3ST1 and/or 3ST2 after infection. To clarify this point, we examined the gene expression in the epithelial fraction of *Ws/Ws* rats, which have a small deletion of the c-kit gene and consequently lack mast cells (35). As shown in Fig. 2, the expression of Relmβ, Siat4c and 3ST1 was upregulated 7 days PI, and that of 3ST2 was upregulated 21 days PI, indicating that mast cells are not relevant to the expression of these genes. These results indicate that the glycosylation status of mucins and/or membrane glycoproteins was modified markedly during the course of infection. Although the precise roles of these changes in inflammatory conditions still remain to be elucidated, some reports have indicated a crucial role of the sialylation and sulfation levels of mucins in *Strongyloides venezuelensis*-infected mice and rats, with the sulfation levels in goblet cells affecting the establishment and distribution of the nematodes in the intestine (36, 37).

Since *N. brasiliensis* larvae reach the small intestine as early as 2–3 days PI, early responses of goblet cell- and mucin glycosylation-related genes after infection were examined. As shown in Fig. 3, MUC2, TFF3 and Siat 4c expression in the jejunal epithelium was upregulated as early as 2–4 days after infection.

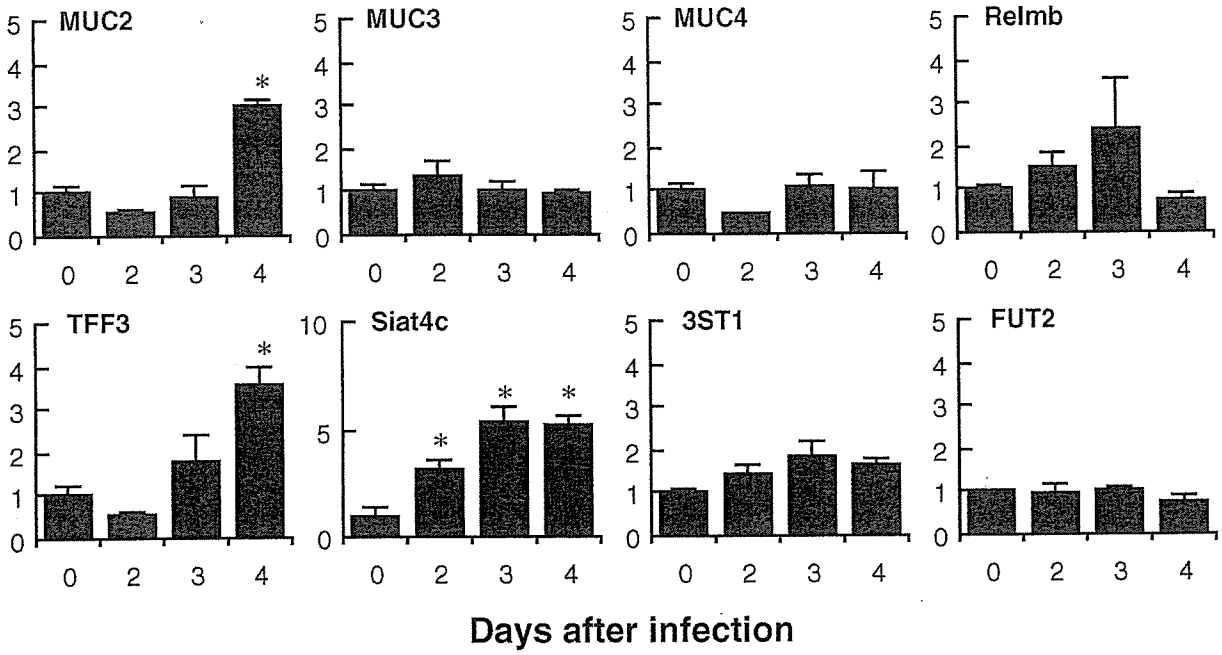

Fig. 3. Expression of goblet cell- and mucin glycosylation-related genes in the jejunal villus epithelium of BN rats in the early period after infection with the nematode *N. brasiliensis*. Total RNA was extracted from the epithelial fraction and semi-quantitative RT-PCR was performed as described in Fig. 1. The data are means+SE of four animals. The vertical axis shows the expression levels, with day-0 average levels expressed as 1.0. *Indicates values significantly different from the day-0 level ($p<0.05$).

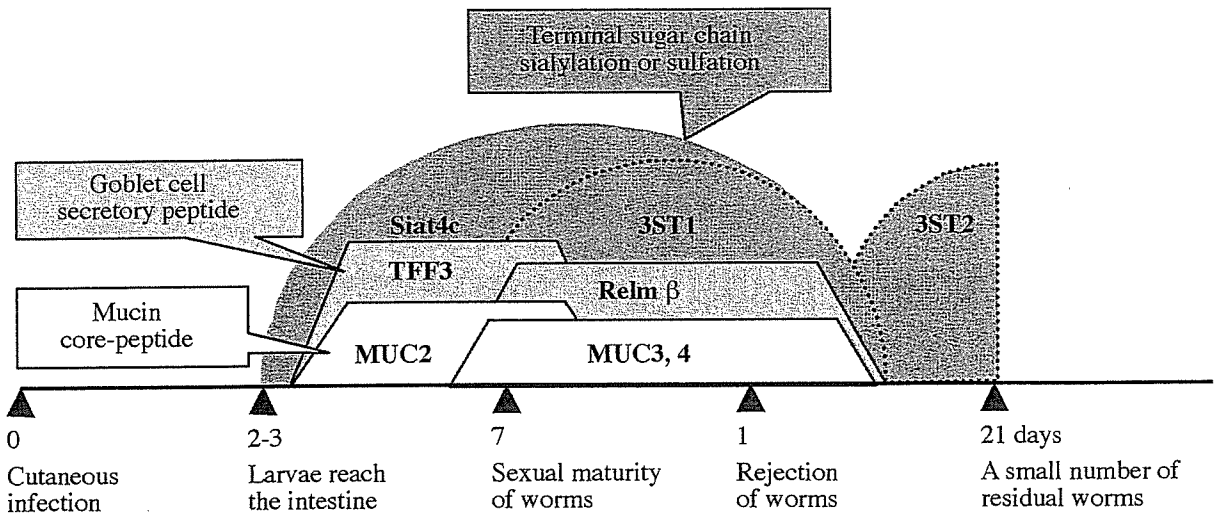

Fig. 4. Successive upregulation of goblet cell- and mucin glycosylation-related genes in the intestinal epithelial cells during the course of *N. brasiliensis* infection.

Taken together, the present findings show that the expression of each goblet cell- and glycosylation-related gene was altered differently during the course of infection (Fig. 4). The early onset of Siat4c, MUC2 and TFF3 gene upregulation might be associated with innate immunity to pathogens or may be related to an acute phase reaction. MUC3, MUC4, Relmβ and 3ST1 gene upregulation, which occurred in the adult-worm colonization and rejection stages, might be regulated by different mechanisms from those of early activated genes, possibly through T-cell-

or Th2 cytokine-dependent acquired immunity. Moreover, the upregulation of sialyl- and sulfotransferase genes suggests that the sialylation and sulfation status of the mucins, membrane glycoproteins and/or histo-blood group antigens might be altered dramatically during nematode infections. The results imply that goblet cell and/or mucin responses to infection are a far more complicated series of changes than previously thought, involving the sequential expression of many factors that can individually or coordinately affect the colonization or rejection of pathogens. Further elucidation of the roles and mechanisms regulating the expression of each mucin and non-mucin secretory peptide and regulating the glycosylation status would lead to development of new strategies for the treatment or prevention of not only intestinal nematode infection but also infection with other pathogens.

This work was supported by a grant-in-aid for scientific research (B16390127) from the Japan Society for the Promotion of Science, and research grants from the Ministry of Health, Labour and Welfare, Japan.

REFERENCES

1. WHO Expert Committee. Prevention and control of schistosomiasis and soil-transmitted helminthiasis. World Health Organization Technical Report Series 2002;912:1–57.
2. Lawrence CE. Is there a common mechanism of gastrointestinal nematode expulsion? Parasite Immunol 2003;25:271–81.
3. Miller HR. Gastrointestinal mucus, a medium for survival and for elimination of parasitic nematodes and protozoa. Parasitology 1987;94: S77–S100.
4. Nawa Y, Ishikawa N, Tsuchiya K, Horii Y, Abe T, Khan AI, et al. Selective effector mechanisms for the expulsion of intestinal helminths. Parasite Immunol 1994;16:333–8.
5. Ogilvie BM, Jones VE. *Nippostrongylus brasiliensis*: a review of immunity and host-parasite relationship in the rat. Exp Parasitol 1971;29:138–77.
6. Ishikawa N, Horii Y, Nawa Y. Immune-mediated alteration of the terminal sugars of goblet cell mucins in the small intestine of *Nippostrongylus brasiliensis*-infected rats. Immunology 1993;78: 303–7.
7. Ishikawa N, Horii Y, Oinuma T, Suganuma T, Nawa Y. Goblet cell mucins as the selective barrier for the intestinal helminths: T-cell-independent alteration of goblet cell mucins by immunologically 'damaged' *Nippostrongylus brasiliensis* worms and its significance on the challenge infection with homologous and heterologous parasites. Immunology 1994;81:480–6.
8. Karlsson NG, Olson FJ, Jovall PA, Andersch Y, Enerback L, Hansson GC. Identification of transient glycosylation alterations of sialylated mucin oligosaccharides during infection by the rat intestinal parasite *Nippostrongylus brasiliensis*. Biochem J 2000;350:805–14.
9. Olson FJ, Johansson ME, Klinga-Levan K, Bouhours D, Enerback L, Hansson GC, et al. Blood group A glycosyltransferase occurring as alleles with high sequence difference is transiently induced during a *Nippostrongylus brasiliensis* parasite infection. J Biol Chem 2002;277:15044–52.
10. Holmen JM, Olson FJ, Karlsson H, Hansson GC. Two glycosylation alterations of mouse intestinal mucins due to infection caused by the parasite *Nippostrongylus brasiliensis*. Glycoconj J 2002;19:67–75.
11. Knight PA, Pemberton AD, Robertson KA, Roy DJ, Wright SH, Miller HR. Expression profiling reveals novel innate and inflammatory responses in the jejunal epithelial compartment during infection with *Trichinella spiralis*. Infect Immun 2004;72:6076–86.
12. Pemberton AD, Knight PA, Gamble J, Colledge WH, Lee JK, Pierce M, et al. Innate BALB/c enteric epithelial responses to *Trichinella spiralis*: inducible expression of a novel goblet cell lectin, intelectin-2, and its natural deletion in C57BL/10 mice. J Immunol 2004;173:1894–901.
13. Audie JP, Janin A, Porchet N, Copin MC, Gosselin B, Aubert JP. Expression of human mucin genes in respiratory, digestive, and reproductive tracts ascertained by in situ hybridization. J Histochem Cytochem 1993;41:1479–85.
14. Matsuoka Y, Pascall JC, Brown KD. Quantitative analysis reveals differential expression of mucin (MUC2) and intestinal trefoil factor mRNAs along the longitudinal axis of rat intestine. Biochim Biophys Acta 1999;1489:336–44.
15. Sheng Z, Wu K, Carraway KL, Fregien N. Molecular cloning of the transmembrane component of the 13762 mammary adenocarcinoma sialomucin complex. A new member of the epidermal growth factor superfamily. J Biol Chem 1992; 267:16341–6.
16. Rong M, Rossi EA, Zhang J, McNeer RR, van den Brande JM, Yasin M, et al. Expression and localization of Muc4/sialomucin complex (SMC) in the adult and developing rat intestine: implications for Muc4/SMC function. J Cell Physiol 2005;202:275–84.
17. Artis D, Wang ML, Keilbaugh SA, He W, Brenes M, Swain GP, et al. RELMbeta/FIZZ2 is a goblet cell-specific immune-effector molecule in the

gastrointestinal tract. Proc Natl Acad Sci U S A. 2004;101:13596–600.
18. Suemori S, Lynch-Devaney K, Podolsky DK. Identification and characterization of rat intestinal trefoil factor: tissue- and cell-specific member of the trefoil protein family. Proc Natl Acad Sci U S A. 1991;88:11017–21.
19. Taupin D, Podolsky DK. Trefoil factors: initiators of mucosal healing. Nat Rev Mol Cell Biol 2003;4:721–32.
20. Hounsell EF, Feizi T. Gastrointestinal mucins. Structures and antigenicities of their carbohydrate chains in health and disease. Med Biol 1982;60:227–36.
21. Delmotte P, Degroote S, Merten MD, Van Seuningen I, Bernigaud A, Figarella C, et al. Influence of TNFalpha on the sialylation of mucins produced by a transformed cell line MM-39 derived from human tracheal gland cells. Glycoconj J 2001;18:487–97.
22. Delmotte P, Degroote S, Lafitte JJ, Lamblin G, Perini JM, Roussel P. Tumor necrosis factor alpha increases the expression of glycosyltransferases and sulfotransferases responsible for the biosynthesis of sialylated and/or sulfated Lewis x epitopes in the human bronchial mucosa. J Biol Chem 2002;277:424–31.
23. Hull SR, Laine RA, Kaizu T, Rodriguez I, Carraway KL. Structures of the O-linked oligosaccharides of the major cell surface sialoglycoprotein of MAT-B1 and MAT-C1 ascites sublines of the 13762 rat mammary adenocarcinoma. J Biol Chem 1984;259:4866–77.
24. Brockhausen I. Sulphotransferases acting on mucin-type oligosaccharides. Biochem Soc Trans 2003;31:318–25.
25. Becker DJ, Lowe JB. Fucose: biosynthesis and biological function in mammals. Glycobiology 2003;13:41R–53R.
26. Isshiki S, Kudo T, Nishihara S, Ikehara Y, Togayachi A, Furuya A, et al. Lewis type 1 antigen synthase (beta3Gal-T5) is transcriptionally regulated by homeoproteins. J Biol Chem 2003;278: 36611–20.
27. Nishida M, Uchikawa R, Tegoshi T, Yamada M, Matsuda S, Sasabe M, et al. Lack of active lung anaphylaxis in congenitally mast cell-deficient *Ws/Ws* rats sensitized with the nematode *Nippostrongylus brasiliensis*. APMIS 1998;106:709–16.
28. Hyoh Y, Ishizaka S, Horii T, Fujiwara A, Tegoshi T, Yamada M, et al. Activation of caspases in intestinal villus epithelial cells of normal and nematode infected rats. Gut 2002;50:71–7.
29. Buisine MP, Devisme L, Savidge TC, Gespach C, Gosselin B, Porchet N, et al. Mucin gene expression in human embryonic and fetal intestine. Gut 1998;43:519–24.
30. Uchikawa R, Yamada M, Matsuda S, Tegoshi T, Nishida M, Kamata I, et al. Dissociation of early and late protective immunity to the nematode *Nippostrongylus brasiliensis* in Brown Norway and Fischer-344 rats. Parasitology 1996;112:339–45.
31. Shekels LL, Anway RE, Lin J, Kennedy MW, Garside P, Lawrence CE, et al. Coordinated Muc2 and Muc3 mucin gene expression in *Trichinella spiralis* infection in wild-type and cytokine-deficient mice. Dig Dis Sci 2001;46:1757–64.
32. Kamal M, Wakelin D, Ouellette AJ, Smith A, Podolsky DK, Mahida YR. Mucosal T cells regulate Paneth and intermediate cell numbers in the small intestine of *T. spiralis*-infected mice. Clin Exp Immunol 2001;126:117–25.
33. Tomita M, Itoh H, Ishikawa N, Higa A, Ide H, Murakumo Y, et al. Molecular cloning of mouse intestinal trefoil factor and its expression during goblet cell changes. Biochem J 1995;311:293–7.
34. Wlad H, Maccarana M, Eriksson I, Kjellen L, Lindahl U. Biosynthesis of heparin. Different molecular forms of O-sulfotransferases. J Biol Chem 1994;269:24538–41.
35. Arizono N, Kasugai T, Yamada M, Okada M, Morimoto M, Tei H, et al. Infection of *Nippostrongylus brasiliensis* induces development of mucosal-type but not connective tissue-type mast cells in genetically mast cell-deficient *Ws/Ws* rats. Blood 1993;81:2572–8.
36. Ishikawa N, Shi BB, Khan AI, Nawa Y. Reserpine-induced sulphomucin production by goblet cells in the jejunum of rats and its significance in the establishment of intestinal helminths. Parasite Immunol 1995;17:581–6.
37. Maruyama H, Hirabayashi Y, el-Malky M, Okamura S, Aoki M, Itagaki T, et al. *Strongyloides venezuelensis*: longitudinal distribution of adult worms in the host intestine is influenced by mucosal sulfated carbohydrates. Exp Parasitol 2002; 100:179–85.

Nucleic Acids Research Advance Access published September 29, 2006

Nucleic Acids Research, 2006, Vol. 00, No. 00 1–9
doi:10.1093/nar/gkl526

An evolutionary 'intermediate state' of mitochondrial translation systems found in *Trichinella* species of parasitic nematodes: co-evolution of tRNA and EF-Tu

Masashi Arita[1], Takuma Suematsu[1,2], Arihiro Osanai[3], Takashi Inaba[3,4], Haruo Kamiya[3], Kiyoshi Kita[2], Masahiko Sisido[1], Yoh-ichi Watanabe[2] and Takashi Ohtsuki[1,*]

[1]Department of Bioscience and Biotechnology, Okayama University, 3-1-1 Tsushimanaka, Okayama 700-8530, Japan, [2]Department of Biomedical Chemistry, The University of Tokyo, 7-3-1 Hongo, Tokyo 113-0033, Japan, [3]Department of Parasitology, Hirosaki University School of Medicine, 5, Zafu-cho, Hirosaki, Aomori 036-8562, Japan and [4]Department of Medical Technology, Hirosaki University, Hriosaki, Aomori 036-8564, Japan

Received May 19, 2006; Revised July 5, 2006; Accepted July 8, 2006

ABSTRACT

EF-Tu delivers aminoacyl-tRNAs to ribosomes in the translation system. However, unusual truncations found in some animal mitochondrial tRNAs seem to prevent recognition by a canonical EF-Tu. We showed previously that the chromadorean nematode has two distinct EF-Tus, one of which (EF-Tu1) binds only to T-armless aminoacyl-tRNAs and the other (EF-Tu2) binds to D-armless Ser-tRNAs. Neither of the EF-Tus can bind to canonical cloverleaf tRNAs. In this study, by analyzing the translation system of enoplean nematode *Trichinella* species, we address how EF-Tus and tRNAs have evolved from the canonical structures toward those of the chromadorean translation system. *Trichinella* mitochondria possess three types of tRNAs: cloverleaf tRNAs, which do not exist in chromadorean nematode mitochondria; T-armless tRNAs; and D-armless tRNAs. We found two mitochondrial EF-Tu species, EF-Tu1 and EF-Tu2, in *Trichinella britovi*. *T.britovi* EF-Tu2 could bind to only D-armless Ser-tRNA, as *Caenorhabditis elegans* EF-Tu2 does. In contrast to the case of *C.elegans* EF-Tu1, however, *T.britovi* EF-Tu1 bound to all three types of tRNA present in *Trichinella* mitochondria. These results suggest that *Trichinella* mitochondrial translation system, and particularly the tRNA-binding specificity of EF-Tu1, could be an intermediate state between the canonical system and the chromadorean nematode mitochondrial system.

INTRODUCTION

Recently, sequencing of metazoan mitochondrial (mt) genomes has proceeded at an accelerated pace. The typical metazoan mt genome is small (14–20 kb) and carries only 37 genes, of which 22 are tRNA genes (1,2). From the mt genome sequences, it has been deduced that mt translation systems of metazoans, particularly invertebrates, include a variety of tRNAs that are truncated as compared to the canonical tRNAs with the common cloverleaf secondary structure (3). Metazoan mt $tRNA^{Ser}$(AGN) genes lack the potential to form the D arm (4), and loss of the T arm has been described for the mt tRNAs from nematodes (5–10), an acanthocephalan (11), trematodes [reviewed in (12)], mollusks (13,14), brachiopods (15,16) and arthropods (17). The most unusual situation occurs in a group of nematodes: the mitochondria of several nematodes of the class Chromadorea (including *Caenorhabditis elegans*, *Ascaris suum* and *Onchocerca volvulus*) have two structurally distinct types of tRNAs, one that lacks the T arm (20 tRNA species) and the other that lacks the D arm (two $tRNAs^{Ser}$) [reviewed in (18–20)]. It has been a mystery how these truncated tRNAs can function in the translation system. In particular, the T arm is necessary for the binding of aminoacyl-tRNAs to the canonical elongation factor Tu (EF-Tu) (21,22). Our recent study showed that a special EF-Tu (EF-Tu1) with an unusual C-terminal extension compensates for the lack of the T arm in *C.elegans* mt tRNAs (23). In *C.elegans* mitochondria, there is a second EF-Tu species (EF-Tu2) that is specific to the serine moiety of Ser-tRNA (24). How have these unique EF-Tu species evolved from the canonical EF-Tu? Understanding how EF-Tu enlargement compensates for tRNA truncation is important for understanding the evolutionary transition from the RNA world to the ribonucleoprotein world.

*To whom correspondence should be addressed. Tel: +81 86 251 8220; Fax: +81 86 251 8219; Email: ohtsuk@cc.okayama-u.ac.jp

Trichinella species, the parasites that cause trichinosis, are classified in the class Enoplea of the phylum Nematoda. It has been reported recently that *Trichinella spiralis* mt DNA contains genes that encode three distinct types of tRNAs: T-armless tRNAs, D-armless tRNAs and cloverleaf tRNAs with a short T arm (25). We therefore postulated that the translation system of *Trichinella* species might be an intermediate evolutionary state between the canonical system that uses only cloverleaf tRNAs and the unusual chromadorean system that uses only tRNAs lacking the T or D arm. In the present study, we confirmed that the *T.spiralis* mt translation system does include at least one cloverleaf tRNA. We cloned two EF-Tu species from *Trichinella britovi*, which is a close relative of *T.spiralis*, and analyzed their aminoacyl-tRNA specificity.

MATERIALS AND METHODS

Parasite

T.britovi, isolated in 1974 (26), was maintained using ICR mice. Muscle larvae were obtained from infected ICR mice by digestion in artificial gastric juice [0.8% (w/v) pepsin and 0.8% (v/v) HCl in physiological saline] for 3 h at 37°C, then washed several times with phosphate-buffered saline (26). The worms were frozen in liquid nitrogen and stored at −80°C until use.

cDNA cloning of *T.britovi* EF-Tu1 and EF-Tu2

The frozen parasitic worms were crushed with a Cryo-Press Frozen Cell Crasher (Microtec, Japan) and poly(A)-plus RNA was prepared with PolyATtract system (Promega). Reverse transcription was carried out with ReverTra Ace (Toyobo, Japan) and random hexamers. The partial cDNA fragment of the putative EF-Tu was obtained by PCR using the degenerate primers P-748 (5′-AC(G,T)AT(A,T)GG(T,C,A,G)CA(T,C)(A,G)T(T,C,A,G)GA(T,C)CA-3′)/P-750 (5′-TC(G,T)G(A,C)(A,G)TG(T,C,A,G)CC(T,C,A,G)GG(A,G)CA(A,G)TC-3′) and P-749 (5′-CA(T,C)(A,G)T(G,T)GA(T,C)CA(T,C)GG(T,C,A,G)AA(A,G)AC-3′)/P-750. The putative cDNA fragments were purified with agarose gel electrophoresis and then cloned using a TOPO TA cloning kit (Invitrogen). Positive clones were screened by colony PCR and sequenced using a DYEnamic ET Terminator Sequencing Kit (GE Healthcare) and a PRISM 310 genetic analyzer (Applied Biosystems). The full-length cDNAs (accession numbers EF-Tu1, AB251621; EF-Tu2, AB251622) were reconstructed from cloned RACE fragments prepared with a GeneRacer kit (Invitrogen) and specific primers (for EF-Tu1, 5′-GCCACGTTTATCGTAATTCCACGGCT-3′ for 5′ RACE, 5′-CGGTAAaACGACACTTACGTCGGCAA-3′ for 3′ RACE; for EF-Tu2, 5′-TTCCTCGTTGTTGCTCTTCTGGTGCTTTGT-3′ and 5′-TGCTCTTCTGGTGCTTTGTCGATTTCGTCG-3′ for 5′ RACE, 5′-CGACGAAATCGACAAAGCACCAGAAGAGCA-3′ and 5′-ACAAAGCACCAGAAGAGCAACAACGAGGAA-3′ for 3′ RACE).

Construction of expression vectors

To construct vectors expressing the EF-Tus with N-terminal thrombin-cleavable His-tags, the putative mature protein-coding regions with 5′ methionine codons were amplified with 5′-CCGcatatgGTGAGCGTAAAAGCTGTTTAC-3′ and 5′-GGGggatccTCATTCCCCTTTCAATTTCAA-3′ for EF-Tu1; and 5′-CCGcatatgGAGTATGAATTGAGCAATACT-3′ and 5′-GGGggatccTCACTGAACTTTCTTTGTTAA-3′ for EF-Tu2 using the cDNA as a template. (NdeI and BamHI sites in the oligos are shown in lower case.) The products were cloned into pGEM-T (Promega) and the sequences were verified. The verified inserts were excised by NdeI and BamHI and then cloned between the NdeI and BamHI sites of pET-15b (Novagen).

Sequence analysis

Sequence alignments were generated with ClustalW version 1.83 (27) followed by manual modification. Based on the alignment, 379 amino acid positions were selected for phylogenetic analysis, with positions of insertion and deletion omitted. Phylogenetic trees were constructed using the maximum-likelihood method of protein phylogeny in the Phyml 2.5 program (28). The WGA + γ model of amino acid substitutions was assumed in the analysis (29,30). Rate heterogeneity among sites was approximated by a discrete gamma distribution (with four categories).

Preparation of the recombinant *T.britovi* mitochondrial EF-Tus

Escherichia coli strain C41 (DE3) or BL21 (DE3) was transformed with the pET-15b-derived expression vector harboring *T.britovi* EF-Tu1 or EF-Tu2 with N-terminal His tags. The transformed cells were grown, harvested by centrifugation and then lysed by sonication and fractionated as described previously (23) with slight modification. Buffer A [50 mM HEPES–KOH (pH 7.5), 150 mM $(NH_4)_2SO_4$, 7 mM $MgCl_2$, 20% glycerol, 15 μM GDP, 7 mM β-mercaptoethanol and 100 μM phenylmethylsulfonyl fluoride] was used to resuspend the cells, Buffer B [50 mM HEPES–KOH (pH 7.5), 1 M NH_4Cl, 10 mM imidazole, 20% glycerol, 1.3 μM GDP and 5 mM β-mercaptoethanol] was used for washing the Ni-NTA column, and Buffer C [50 mM HEPES–KOH (pH 7.5), 100 mM $(NH_4)_2SO_4$, 150 mM imidazole, 20% glycerol, 2 μM GDP and 5 mM β-mercaptoethanol] was used for eluting the His-tagged protein. The obtained protein was treated with biotinylated thrombin during dialysis to digest the His tag at the N-terminus and was purified with streptavidin agarose.

Preparation of tRNAs

A.suum mt $tRNA^{Lys}$ was purified from *A.suum* as described previously (31). All other tRNAs used in this study were prepared by *in vitro* transcription. To generate DNA templates for the transcription, primer extension reactions were performed using KOD Dash DNA polymerase (TOYOBO) and two primers designed to complement each other at their 3′ regions (~20 nt). In the DNA templates, the promoter sequence for T7 RNA polymerase was directly connected to the upstream region of the tRNA sequence. The transcription reaction was performed at 37°C for 4 h in a reaction mixture that included 40 mM Tris–HCl (pH 8.0), 6 mM $MgCl_2$, 5 mM DTT, 1 mM spermine, 0.01% Triton X-100, 50 μg/ml BSA, 10 mM GMP, 0.5 mM each of ATP, GTP, CTP and UTP, 90 μg/ml T7 RNA polymerase and 10 μg/ml template

DNA. For *T.spiralis* mt $tRNA^{Trp}$, which bears an A at its 5′ end, a hammerhead ribozyme sequence was introduced between the T7 RNA polymerase promoter and the tRNA sequence in the transcription template, and its transcript was cleaved by the ribozyme to separate the $tRNA^{Trp}$ and the ribozyme according to a method described previously (32). The products were purified by 10% denaturing PAGE.

Enzymatic probing of tRNA

Enzymatic probing of *T.spiralis* $tRNA^{Trp}$ was performed according to a method described previously (8). 5′-^{32}P-labeled tRNAs were digested with RNase T_2 (2.5×10^{-5} or 6×10^{-6} U) or RNase V_1 (0.09 or 0.0225 U) in 5 µl of 50 mM sodium acetate (pH 6.0) and 10 mM $MgCl_2$. The digestion was performed at 37°C for 7 min.

Preparation of aminoacyl-tRNAs using aminoacyl-tRNA synthetases

Bovine mt Ser- or Ala-$tRNA^{Ser}$ was prepared as described previously (33). Mitochondrial [^{3}H]Lys-$tRNAs^{Lys}$ of *T.spiralis* and *A.suum*, and *Drosophila melanogaster* mt [^{35}S]Cys-$tRNA^{Cys}$ were prepared using recombinant *C.elegans* putative mt lysyl-tRNA synthetase (LysRS) and putative mt cysteinyl-tRNA synthetase (CysRS), respectively. *C.elegans* LysRS and CysRS were expressed in *E.coli* Rosetta (DE3) (Novagen) using expression vectors derived from pET-28b (Novagen) and prepared using cDNA clone yk468a3 for LysRS and cDNA clone yk79g12 for CysRS, which were kindly provided by Prof. Y. Kohara. Aminoacylation reactions were performed at 37°C for 30 min in a reaction mixture that contained 50 mM HEPES–KOH (pH 7.8), 10 mM $MgCl_2$, 1 mM spermine, 20 mM KCl, 2.5 mM ATP, 2 mM DTT, 30 µM [^{3}H]lysine (74 Bq/pmol) or [^{35}S]cysteine (39.8 kBq/pmol), 320µg/ml aminoacyl-tRNA synthetase (ARS) and 0.002–0.005 A_{260}unit/µl of tRNA. The aminoacyl-tRNAs were purified as described previously (23) and finally dissolved in 6 mM KOAc (pH 5.0) at a concentration of 2 µM. The concentration of aminoacyl-tRNA was estimated from the labeled amino acids incorporated into the tRNA.

Chemical aminoacylation

Phe-$tRNA^{Lys}$ and Phe-$tRNA^{Trp}$ of *T.spiralis* mitochondria were prepared by ligating the tRNA transcript without the 3′-CA sequence and the phenylalanyl-dinucleotide (p2′dCpA-Phe) with T4 RNA ligase as described previously (34,35). The purified Phe-tRNAs were dissolved with 6 mM KOAc (pH 5.0).

Hydrolysis protection assay

The assay was basically performed according to the method described in Refs (36,23). The deacylation reaction mixture contained 75 mM Tris–HCl (pH 7.5), 75 mM NH_4Cl, 15 mM $MgCl_2$, 7.5 mM DTT, 60 mg/ml BSA, 0.1 mM GTP, 2.375 mM phosphoenolpyruvate, 2.5 U/ml pyruvate kinase, 1.2 µM EF-Tu and 0.2 µM aminoacyl-tRNA. The reaction mixture was preincubated at 30°C for 10 min without aminoacyl-tRNA, after which aminoacyl-tRNA was added. The deacylation reaction was performed at 30°C.

Gel mobility shift assay

The ternary complex of *T.britovi* EF-Tu1, GTP and aminoacyl-tRNA was prepared as follows. The binary complex of EF-Tu1 and GTP was prepared at 30°C for 10 min in 12 µl of a reaction mixture containing 2.4 mM Tris–HCl (pH 6.8), 3 mM NH_4OAc, 0.5 mM $Mg(OAc)_2$, 5 mM GTP, 50 mM phosphoenolpyruvate, 0.05 U/µl pyruvate kinase and 24 µM EF-Tu1. To this solution, 0.1 A_{260} unit of aminoacyl-tRNA was added, and the resulting mixture was incubated at 4°C for 10 min. Electrophoresis of the samples was carried out in 5% polyacrylamide gels at room temperature for 30 min at 50 V in a buffer containing 50 mM Tris–HCl (pH 8.0), 65 mM NH_4OAc, 10 mM $Mg(OAc)_2$ and 1 mM EDTA (pH 8.0). The gel was stained with ethidium bromide.

RESULTS

Sequences of *T.britovi* EF-Tu1 and EF-Tu2

Using cDNA cloning and sequencing of *T.britovi* EF-Tu, we found two EF-Tu homologues (EF-Tu1 and EF-Tu2). The amino acid sequence of *T.britovi* EF-Tu1 had 56% homology to that of *C.elegans* EF-Tu1 (Figure 1B). The T stem-binding residues commonly seen in canonical EF-Tu (21,22) were not conserved at all in *T.britovi* EF-Tu1, which had a C-terminal extension that is not seen in canonical EF-Tus (Figure 1B). Although the C-terminal extension of *T.britovi* EF-Tu1 (41 residues) is shorter than that of *C.elegans* EF-Tu1 (57 residues), these features of *T.britovi* EF-Tu1 do resemble those of *C.elegans* EF-Tu1, suggesting that *T.britovi* EF-Tu1 may recognize T-armless tRNAs, as *C.elegans* EF-Tu1 does (23). The amino acid sequence of *T.britovi* EF-Tu2 was significantly homologous (47%) to that of *C.elegans* EF-Tu2. *T.britovi* EF-Tu2 had a relatively short C-terminal extension (18 residues), similar to *C.elegans* EF-Tu2. In Figure 1B, the asterisks show the residues involved in the side-chain pocket of the aminoacyl group, which has been reported for canonical EF-Tu (21,22). At these positions, *T.britovi* EF-Tu2 was homologous to *C.elegans* EF-Tu2 but not to *Thermus thermophilus* EF-Tu (Figure 1B). Thus, *T.britovi* EF-Tu2 may be specific for the seryl group of seryl-tRNAs, as *C.elegans* EF-Tu2 is.

Secondary structure of *T.spiralis* mt $tRNA^{Trp}$

T.spiralis (Nematoda: Enoplea) mt DNA has been reported to encode three types of tRNAs, T-armless tRNAs, cloverleaf tRNAs with a short T arm and D-armless tRNAs (25), whereas mitochondria of chromadorean nematodes (e.g. *C.elegans*, *A.suum* and *O.volvulus*) do not have any cloverleaf tRNAs (5,7,9). To confirm that *T.spiralis* has cloverleaf tRNAs in its mitochondria, we analyzed the secondary structure of *T.spiralis* mt $tRNA^{Trp}$, which has been suggested to be a cloverleaf tRNA (37), in an enzymatic probing experiment. The digestion pattern is shown in Figure 2A and the results are summarized in Figure 2B. The digestion pattern shows that double strand-specific RNase V_1 cleaved the T stem region and single strand-specific RNase T_2 cleaved the T-loop region. These observations indicate the $tRNA^{Trp}$ has a T arm and thus is a cloverleaf tRNA.

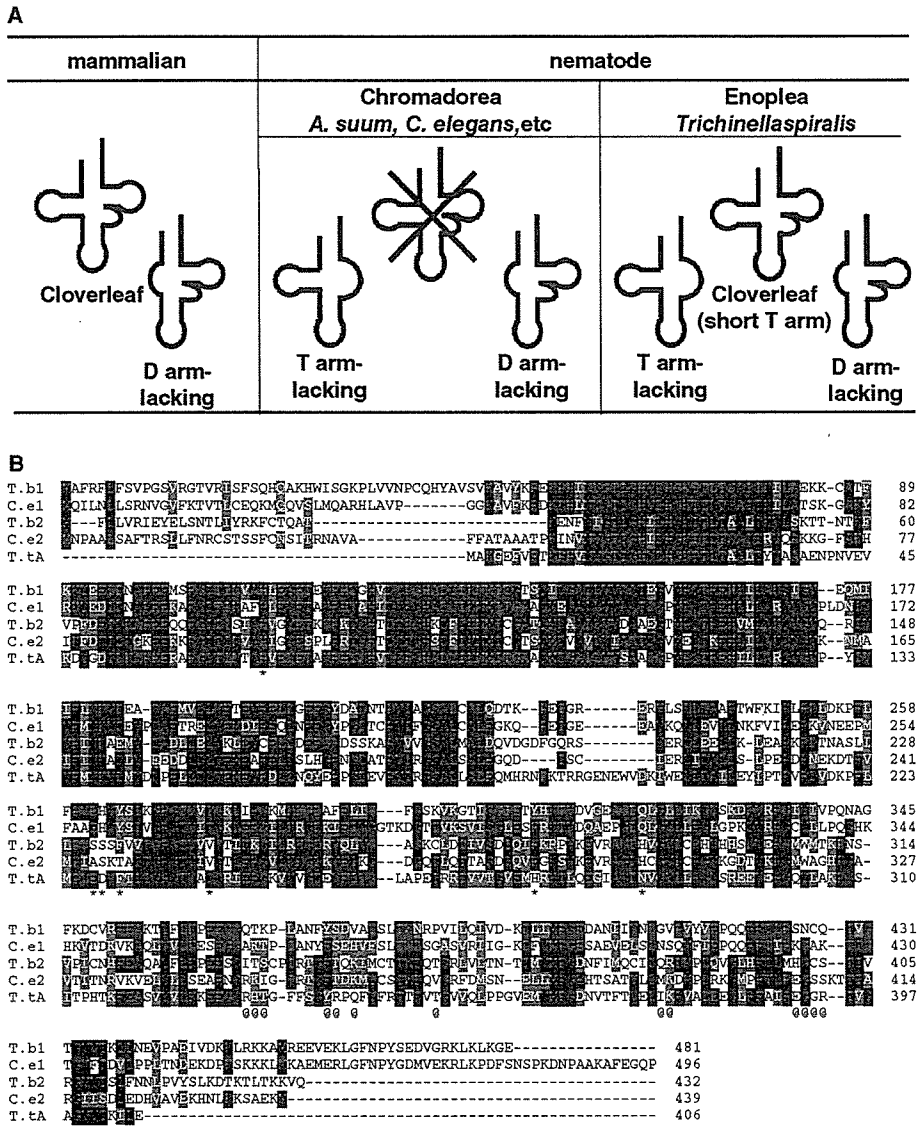

Figure 1. Characteristic features of *T.spiralis* mt tRNAs and *T.britovi* mt EF-Tus. (**A**) Secondary structures of mitochondrial tRNAs of the enoplean nematode *T.spiralis*, chromadorean nematodes and mammals. (**B**) Alignment of mitochondrial EF-Tus of *T.britovi* EF-Tu1 (T.b1, this study, accession no. AB251621), *T.britovi* EF-Tu2 (T.b2, this study, accession no. AB251622), *C.elegans* EF-Tu1 (C.e1, accession no. BAA07491) and *C.elegans* EF-Tu2 (C.e2, accession no. BAA31345), together with *T.thermophilus* EF-Tu (T.tA, Q5SHN6). The alignment was modified using BoXSHADE (http://www.ch.embnet.org/software/BOX_form.html). The black and gray shadings indicate identical and similar amino acid sequences, respectively. Asterisks indicate the residues involved in the side-chain pocket of the aminoacyl group, and '@' indicates the residues in contact with the T stem (21,22).

Trichinella EF-Tu1 binds to three types of tRNAs

To analyze the binding of *T.britovi* EF-Tus to T-armless tRNAs and to tRNAs with a short T arm, we first performed deacylation protection assays (36), in which the spontaneous deacylation rate of an aminoacyl-tRNA is suppressed when an EF-Tu binds to it. We employed native *A.suum* mt $tRNA^{Lys}$ and transcripts of *T.spiralis* mt $tRNA^{Lys}$ and *D.melanogaster* mt $tRNA^{Cys}$ in this assay (Figure 3A–C). *A.suum* mt $tRNA^{Lys}$ was used as an example of a T-armless tRNA. *D.melanogaster* mt $tRNA^{Cys}$ has a structure similar to the cloverleaf tRNAs of *T.spiralis* mitochondria, whose T arms are shorter than those of canonical tRNAs. Although *T.spiralis* mt $tRNA^{Lys}$ has been classified as a cloverleaf tRNA (37), it would seem difficult for this tRNA to form a stable T arm because the hypothetical T arm contains only 2 bp with a 4 base loop. The result of the enzymatic probing experiment implied that no T stem was formed in this tRNA (data not shown); this is not unusual, because more than half of *T.spiralis* mt tRNAs lack the T arm (37). About 14% of *T.spiralis* mt $tRNA^{Lys}$ and 41% of *A.suum* mt $tRNA^{Lys}$ were lysylated by *C.elegans* mt LysRS, and 12% of *D.melanogaster* $tRNA^{Cys}$ was charged with cysteine

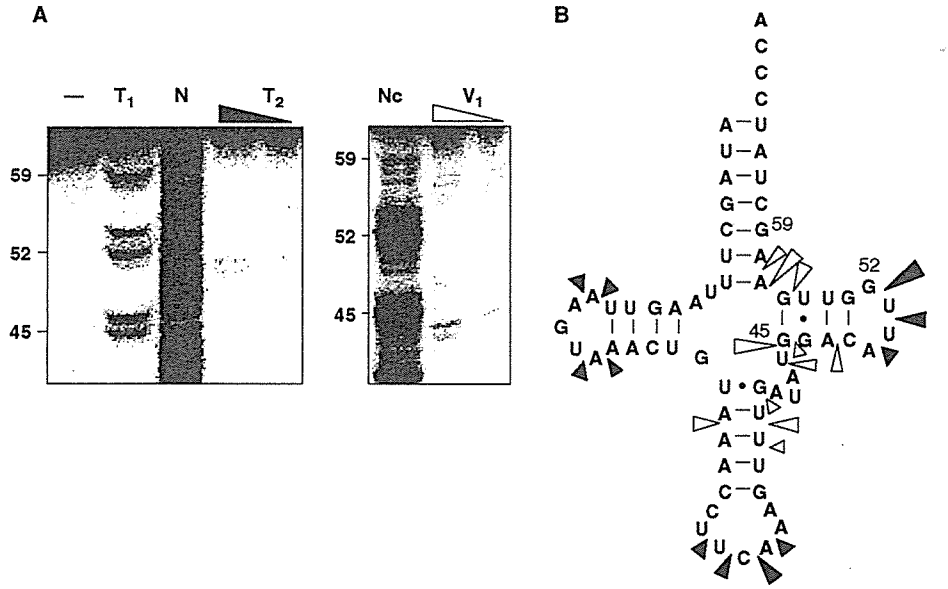

Figure 2. Enzymatic probing of 5′-labeled *T.spiralis* mt $tRNA^{Trp}$. (**A**) 5′-Labeled $tRNA^{Trp}$ was reacted with 2.5×10^{-5} or 6×10^{-6} U of RNase T_2 and 0.09 or 0.0225 U of RNase V_1. The closed and open triangles indicate the decreasing amounts of RNase T_2 and V_1, respectively. Symbols: dash, untreated tRNA; N, alkaline ladder; T_1, RNase T_1 ladder; and Nc, ladder of digestion with *Neurospora crassa* endonuclease as a size marker for RNase V_1, which digests at the 5′ side of phosphodiester bonds. (**B**) Secondary structure of *T.spiralis* mt $tRNA^{Trp}$. Closed and open triangles indicate the cleavage sites with RNase T_2 and RNase V_1, respectively. The cleavage strengths are shown by the triangle sizes. The 3mer at the 5′ end and 8mer at the 3′ end were not analyzed.

by *C.elegans* mt CysRS. *T.britovi* EF-Tu1 bound to the T-armless tRNAs and to the tRNA with a short T arm but EF-Tu2 did not (Figure 3D–F). The tRNA specificity of *T.britovi* EF-Tu1 was different from that of *C.elegans* EF-Tu1 in that *T.britovi* EF-Tu1 bound the tRNA with a short T arm but *C.elegans* EF-Tu1 did not.

The binding of *T.britovi* EF-Tu1 to the three types of tRNAs was also analyzed with a gel mobility shift assay (Figure 4). In this assay, we used *T.spiralis* mt Phe-$tRNA^{Trp}$ as a cloverleaf tRNA with a short T arm (Figure 2), *T.spiralis* mt Phe-$tRNA^{Lys}$ as a T-armless tRNA (Figure 3B) and bovine mt Ser-$tRNA^{Ser}_{GCU}$ as a D-armless tRNA (Figure 5A). The $tRNA^{Trp}$ and $tRNA^{Lys}$ were chemically aminoacylated using p2′dCpA-Phe because ARSs did not aminoacylate these tRNAs efficiently enough for a gel-shift assay. The gel-mobility shift assay shows that all three of these aminoacyl-tRNAs bound to EF-Tu1 (Figure 4). The uncharged tRNAs (*T.spiralis* mt $tRNA^{Trp}$ and $tRNA^{Lys}$, and bovine mt $tRNA^{Ser}_{GCU}$) did not bind to *T.britovi* EF-Tu1 (Supplementary Figure 2). The binding of the D-armless Ser-tRNA to *T.britovi* EF-Tu1 (Figure 5B) was unexpected because *C.elegans* EF-Tu1 does not bind to D-armless tRNAs (24). We also found that the EF-Tu1 could bind to cloverleaf tRNAs only if they had a short T arm, and could not bind to canonical cloverleaf tRNAs (Supplementary Figure 1).

Trichinella EF-Tu2 binds to D-armless Ser-tRNA but not to D-armless Ala-tRNA

Our previous study showed that *C.elegans* EF-Tu2 exclusively recognizes the serine moiety of Ser-tRNA (24). In this study, we investigated whether *T.britovi* EF-Tu2 also has serine specificity. In this assay, a bovine mt $tRNA^{Ser}_{GCU}$ mutant (Figure 5A) was used because this tRNA can be charged with Ser by bovine mt seryl-tRNA synthetase and also with Ala by *E.coli* alanyl-tRNA synthetase (24). A deacylation protection assay was performed with *T.britovi* EF-Tu2 using either Ser-tRNA or Ala-tRNA (Figure 5). The tRNA bodies of the Ser-tRNA and Ala-tRNA are entirely the same. *T.britovi* EF-Tu2 bound to the Ser-tRNA but not to the Ala-tRNA (Figure 5B and C), whereas bovine mt EF-Tu and *T.britovi* EF-Tu1 bound to both Ser-tRNA and Ala-tRNA. This suggests that *T.britovi* EF-Tu2 is serine-specific, like *C.elegans* EF-Tu2. However, the esterified serine cannot be the only criterion for *T.britovi* EF-Tu2 binding; the tRNA part must also be important as *E.coli* Ser-$tRNA^{Ser}$ failed to bind to EF-Tu2 (Supplementary Figure 1). In the case of bacterial EF-Tu, it is known that both the esterified amino acid and the tRNA part of the aminoacyl-tRNA contribute to the binding affinity of EF-Tu (38).

DISCUSSION

The lack of a T or D arm in some mt tRNAs seems to be related to the small size of the mt genome. However, the lack of a T arm requires some functional support, because the T arm is necessary for binding EF-Tu in the canonical translation system. Canonical EF-Tus, such as bacterial EF-Tu, can bind to canonical cloverleaf-type tRNA and D-armless tRNA (39) but not to T-armless tRNA (23). In contrast, EF-Tu1 from chromadorean nematodes binds specifically to T-armless tRNAs and cannot bind to cloverleaf tRNA (23). To understand the evolutionary process that has generated the T-armless tRNA, it is necessary to investigate

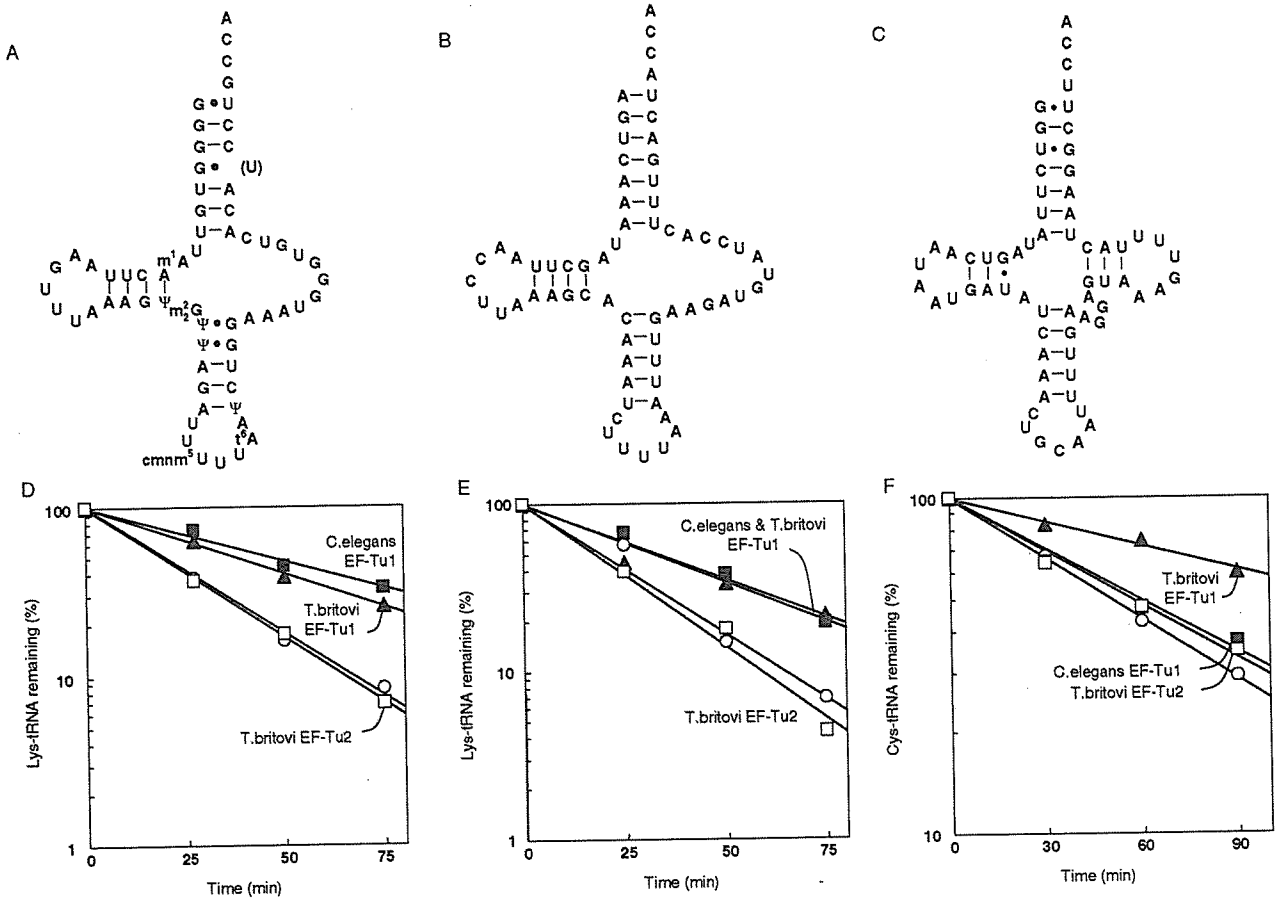

Figure 3. Binding of EF-Tu1 and EF-Tu2 to T-armless and cloverleaf (short T arm) tRNAs. (A–C) Sequences and secondary structures of (A) *A.suum* mt $tRNA^{Lys}$ (5), (B) *T.spiralis* mt $tRNA^{Lys}$ (37) and (C) *D.melanogaster* mt $tRNA^{Cys}$ (43). (D–F) Deacylation-protection assay using (D) *A.suum* mt Lys-$tRNA^{Lys}$, (E) *T.spiralis* mt Lys-$tRNA^{Lys}$ and (F) *D.melanogaster* mt Cys-$tRNA^{Cys}$. These assays were performed in the presence of *T.britovi* EF-Tu1 (closed triangles), *T.britovi* EF-Tu2 (open squares), *C.elegans* EF-Tu1 (closed squares) and in the absence of EF-Tu (open circles).

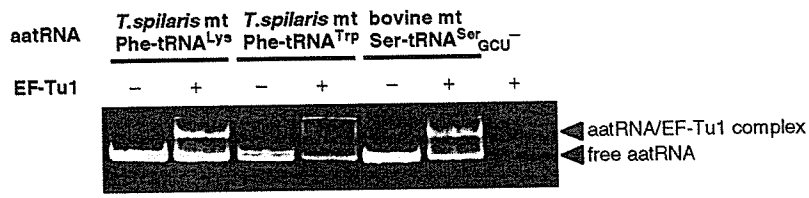

Figure 4. Binding of EF-Tu1 to three types of aminoacyl-tRNAs. *T.spiralis* mt Phe-$tRNA^{Lys}$, *T.spiralis* mt Phe-$tRNA^{Trp}$ and bovine mt Ser-$tRNA^{Ser}$ in the presence or absence of EF-Tu1 were analyzed by gel mobility shift assay under the conditions described in Materials and Methods. The gel was stained with ethidium bromide.

how EF-Tu co-evolved with tRNAs, including how the division of labor arose between the two EF-Tus of *C.elegans*, EF-Tu2 for the two D-armless $tRNAs^{Ser}$ and EF-Tu1 for the other 20 T-armless tRNAs (24), given the ability of the canonical EF-Tu to deliver all elongator tRNAs. In this study, we found in *Trichinella* spp. an intermediate state in the evolutionary process that generates EF-Tu for T-armless tRNAs and divides the labor between different EF-Tus.

In this study, we found that the EF-Tu1 from the enoplean nematode *T.britovi* bound to all three types of tRNAs that exist in *Trichinella* mitochondria: T-armless tRNAs, D-armless tRNAs and cloverleaf tRNAs with a short T arm (Figures 4 and 6). *T.britovi* EF-Tu1 thus seems to be in the evolutionary midstream between canonical EF-Tu and the chromadorean nematode EF-Tu1 that specifically binds to T-armless tRNA. *T.britovi* EF-Tu1 has a C-terminal extension of 41 residues compared to the canonical EF-Tu; this is shorter by 16 residues than that of *C.elegans* EF-Tu1, but the extension is 44% homologous to the N-terminal 41 residues of the C-terminal extension of *C.elegans* EF-Tu1.

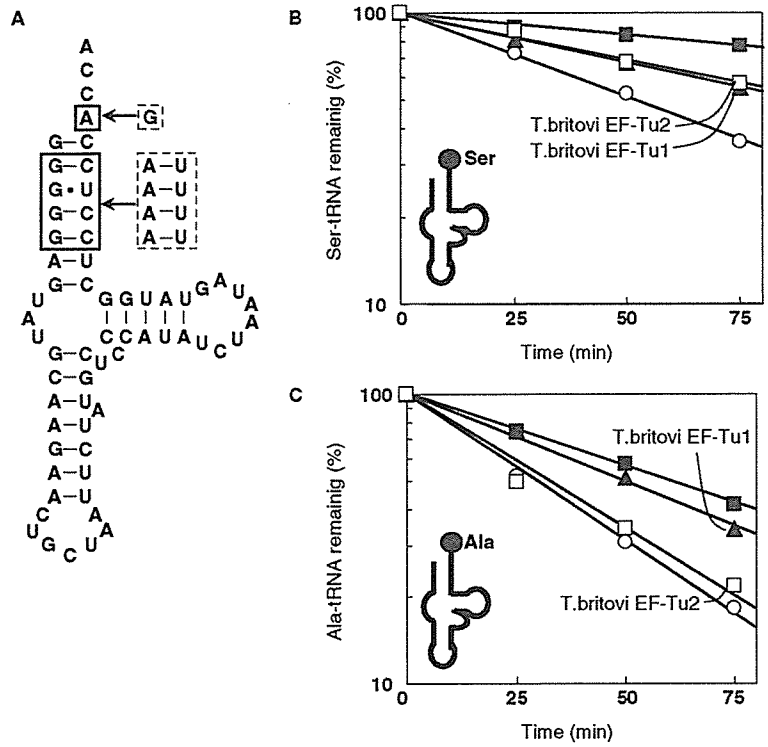

Figure 5. Serine specificity of EF-Tu2. (**A**) The secondary structure of the bovine mt $tRNA^{ser}_{GCU}$ derivative with alanine identity. The mutated residues are enclosed within the solid lines. For the mutated positions, the native sequence of $tRNA^{Ser}$ is shown within the dotted lines. Deacylation protection assays using Ser-tRNA (**B**) and Ala-tRNA (**C**) were performed with bovine mt EF-Tu (closed squares), *T.britovi* EF-Tu1 (closed triangles), *T.britovi* EF-Tu2 (open squares) and in the absence of EF-Tu (open circles).

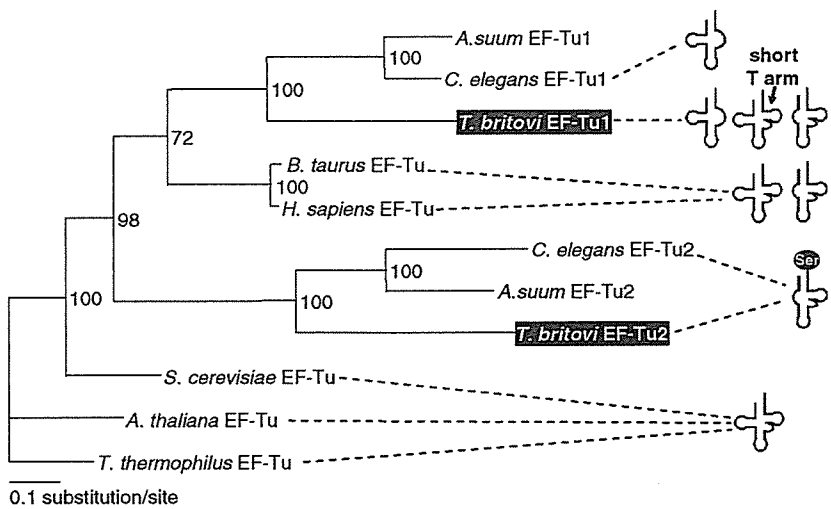

Figure 6. Phylogenetic representation of tRNA recognition patterns of mitochondrial EF-Tus. Numbers on branches are the bootstrap values from 100 pseudo datasets. The sequences are those shown in Figure 1, plus *Homo sapiens* (accession no. X84694), *Bos taurus* (L38996), *A.suum* (EF-Tu1, AB211994; EF-Tu2, AB212082), *S.cerevisiae* (K00428) and *A.thaliana* (X89227). Dotted lines show the tRNA specificity of each EF-Tu.

Although determination of the tertiary structure will be necessary to clarify the tRNA-recognition mechanism of *T.britovi* EF-Tu1, the following mechanism is suggested by the present and previous studies. *T.britovi* EF-Tu1 binds to cloverleaf tRNAs with a short T arm (Figure 4) but not to canonical cloverleaf tRNAs (Supplementary Figure 1). This specificity is not strange for *T.britovi* EF-Tu1 because *Trichinella* species do not have any canonical cloverleaf

tRNAs (25). Cloverleaf tRNAs with a short T arm do not have the conserved residues present in canonical tRNAs that are responsible for T arm–D arm interactions (40). RNase T_2 digested most of the T-loop and D-loop regions of *T.spiralis* mt $tRNA^{Trp}$ (Figure 2), indicating that the tRNA does not have T arm–D arm interactions. *T.britovi* EF-Tu1 can discriminate between cloverleaf tRNAs having a normal T-arm and a short T-arm because it may recognize a part of the tRNA that is hidden by the T arm–D arm interaction. The C-terminal extension of *T.britovi* EF-Tu1 probably has a role in recognizing T-armless tRNA, similar to the role of the C-terminal extension of *C.elegans* EF-Tu1 (23). That the C-terminal extension of *T.britovi* EF-Tu1 is shorter by 16 residues than that of *C.elegans* EF-Tu1 may explain why *T.britovi* EF-Tu1 can bind to a cloverleaf tRNA with a short T arm whereas *C.elegans* EF-Tu1 cannot (Figure 3F).

The length of the C-terminal extension of EF-Tu is likely to have co-evolved with the length of the T arm of tRNA; the shorter the T arm, the longer the C-terminal extension becomes. In mammalian mitochondria, EF-Tu has an 11 amino acid C-terminal extension (41) that can recognize canonical cloverleaf tRNAs and tRNAs with a short T arm, such as those containing a 4 bp T stem or a 4 nt T loop. In mitochondria of the enoplean nematode *T.britovi*, EF-Tu1, which bears a 41 amino acid C-terminal extension, can bind tRNAs with a short T arm or no T arm. In the chromadorean nematode *C.elegans*, EF-Tu1, which has a 57 amino acid C-terminal extension, can bind only to T-armless tRNAs. No animal mt translation systems known so far contradict this hypothetical rule.

In the mitochondria of both *C.elegans* and *Trichinella*, the only tRNAs for serine are two D-armless tRNAs (7,25). *C.elegans* EF-Tu2 specifically recognizes the serine moiety of Ser-tRNA, and thus it can bind only to tRNA charged with serine (24). As shown in Figure 5, *T.britovi* EF-Tu2 has the same serine specificity, suggesting that this unique recognition mechanism was established at the common ancestor of Chromadorea and Enoplea and likely persists due to the conservation of the secondary structure of two $tRNAs^{Ser}$, at least in nematodes.

Plants (e.g. *Arabidopsis thaliana*) and fungi (e.g. *Saccharomyces cerevisiae*) have only a single mt EF-Tu, which is closely related to the bacterial EF-Tu (Figure 6), suggesting that mt EF-Tu was highly homologous to the canonical EF-Tu when mitochondria were generated from the ancestral bacteria. It is likely that the mt EF-Tu gene was duplicated after the emergence of the metazoa (Figure 6), and then the two EF-Tu genes co-evolved with different types of truncated tRNAs into distinct forms. However, the mt translation systems of some lineages, such as mammals (bovine, Figure 6), have only a single EF-Tu, which is structurally close to the canonical EF-Tu (41,42). Thus, it is likely that duplication of the EF-Tu gene and the unique evolution of EF-Tus have occurred in some lineage(s), including that of nematodes, but not in others. From a functional standpoint, unique EF-Tu species are not necessary in mammalian mitochondria, which contain only moderately truncated tRNAs. The duplication of the EF-Tu gene and the independent evolution of the duplicated genes probably contributed to the extreme truncation of nematode mt tRNAs.

The evolutionary process from canonical EF-Tu to chromadorean nematode EF-Tus has not been well known. In this study, we clarified the connection between the two EF-Tu species and three types of tRNAs in *Trichinella* spp. Our data suggest that enoplean EF-Tu1 is an evolutionary intermediate between the canonical EF-Tu and the chromadorean nematode EF-Tu1 for T-armless tRNAs. Furthermore, the present study of the *Trichinella* system gives insight into how the division of labor by two EF-Tus in *C.elegans* was established. In *T.britovi*, EF-Tu1 can bind all three of the mt tRNA types present in this organism and can deliver all elongator aminoacyl-tRNAs; it therefore seems that EF-Tu2, which binds only to Ser-tRNAs, is an auxiliary factor in the *T.britovi* mt translation system. The *T.britovi* system thus represents a transition state from the canonical system, which requires only a single EF-Tu, to the *C.elegans* system, which requires two distinct EF-Tus. To understand this co-evolutionary process in detail, it will be necessary to analyze tRNA sequences, EF-Tu sequences and tRNA-recognition specificities of EF-Tu for various metazoan species. Understanding how protein enlargement compensates for RNA truncations will be quite important for considering the transition from RNA world to the ribonucleoprotein world.

SUPPLEMENTARY DATA

Supplementary Data are available at NAR Online.

ACKNOWLEDGEMENTS

We thank Dr A. Sato (University of Tokyo) for *D.melanogaster* mt $tRNA^{Cys}$, and Prof. Y. Kohara (National Institute of Genetics, Japan) for the cDNA clones. This work was supported by the Kurata Memorial Hitachi Science and Technology Foundation to T. O. and JSPS to Y. W. Funding to pay the Open Access publication charges for this article was provided by JSPS.

Conflict of interest statement. None declared.

REFERENCES

1. Boore,J.L. (1999) Animal mitochondrial genomes. *Nucleic Acids Res.*, **27**, 1767–1780.
2. Lynch,M., Koskella,B. and Schaack,S. (2006) Mutation pressure and the evolution of organelle genomic architecture. *Science*, **311**, 1727–1730.
3. Sprinzl,M. and Vassilenko,K.S. (2005) Compilation of tRNA sequences and sequences of tRNA genes. *Nucleic Acids Res.*, **33**, D139–D140.
4. Wolstenholme,D.R. (1992) Animal mitochondrial DNA: structure and evolution. In Wolstenholme,D.R. and Jeon,K.W. (eds), *Mitochondrial Genomes*. Academic Press, NY, pp. 173–216.
5. Wolstenholme,D.R., Macfarlane,J.L., Okimoto,R., Clary,D.O. and Wahleithner,J.A. (1987) Bizarre tRNAs infered from DNA sequences of mitochondrial genomes of nematode worms. *Proc. Natl Acad. Sci USA*, **84**, 1324–1328.
6. Okimoto,R. and Wolstenholme,D.R. (1990) A set of tRNAs that lack either the TyC arm or dihydrouridine arm: towards a minimal tRNA adaptor. *EMBO J.*, **9**, 3405–3411.
7. Okimoto,R., Macfarlane,J.L., Clary,D.O. and Wolstenholme,D.R. (1992) The mitochondrial genomes of two nematodes, *Caenorhabditis elegans* and *Ascaris suum*. *Genetics*, **130**, 471–498.
8. Watanabe,Y., Tsurui,H., Ueda,T., Furushima,R., Takamiya,S., Kita,K., Nishikawa,K. and Watanabe,K. (1994) Primary and higher order

structures of Nematode (*Ascaris suum*) mitochondrial tRNAs lacking either the T or D stem. *J. Biol. Chem.*, **269**, 22902–22906.
9. Keddie,E.M., Higazi,T. and Unnasch,T.R. (1998) The mitochondrial genome of *Onchocerca volvulus*: sequence, structure and phylogenetic analysis. *Mol. Biochem. Parasitol.*, **95**, 111–127.
10. Hu,M., Chilton,N.B. and Gasser,R.B. (2002) The mitochondrial genomes of the human hookworms, *Ancylostoma duodenale* and *Necator americanus* (Nematoda: Secernentea). *Int. J. Parasitol.*, **32**, 145–158.
11. Steinauer,M.L., Nickol,B.B., Broughton,R. and Orti,G. (2005) First sequenced mitochondrial genome from the phylum Acanthocephala (*Leptorhynchoides thecatus*) and its phylogenetic position within Metazoa. *J. Mol. Evol.*, **60**, 706–715.
12. Le,T.H., Blair,D. and McManus,D.P. (2002) Mitochondrial genomes of parasitic flatworms. *Trends Parasitol.*, **18**, 206–213.
13. Terrett,J.A., Miles,S. and Thomas,R.H. (1996) Complete DNA sequence of the mitochondrial genome of *Cepaea nemoralis* (Gastropoda: Pulmonata). *J. Mol. Evol.*, **42**, 160–168.
14. Yamazaki,N., Ueshima,R., Terrett,J.A., Yokobori,S., Kaifu,M., Segawa,R., Kobayashi,T., Numachi,K., Ueda,T., Nishikawa,K. *et al.* (1997) Evolution of pulmonate gastropod mitochondrial genomes: comparisons of gene organizations of Euhadra, Cepaea and Albinaria and implications of unusual tRNA secondary structures. *Genetics*, **145**, 749–758.
15. Noguchi,Y., Endo,K., Tajima,F. and Ueshima,R. (2000) The mitochondrial genome of the brachiopod *Laqueus rubellus*. *Genetics*, **155**, 245–259.
16. Helfenbein,K.G., Brown,W.M. and Boore,J.L. (2001) The complete mitochondrial genome of the articulate brachiopod *Terebratalia transversa*. *Mol. Biol. Evol.*, **18**, 1734–1744.
17. Masta,S.E. and Boore,J.L. (2004) The complete mitochondrial genome sequence of the spider *Habronattus oregonensis* reveals rearranged and extremely truncated tRNAs. *Mol. Biol. Evol.*, **21**, 893–902.
18. Hu,M. and Gasser,R.B. (2006) Mitochondrial genomes of parasitic nematodes—progress and perspectives. *Trends Parasitol.*, **22**, 78–84.
19. Kim,K.H., Eom,K.S. and Park,J.K. (2006) The complete mitochondrial genome of *Anisakis simplex* (Ascaridida: Nematoda) and phylogenetic implications. *Int. J. Parasitol.*, **36**, 319–328.
20. Montiel,R., Lucena,M.A., Medeiros,J. and Simoes,N. (2006) The complete mitochondrial genome of the entomopathogenic Nematode *Steinernema carpocapsae*: insights into Nematode mitochondrial DNA evolution and phylogeny. *J. Mol. Evol.*, **62**, 211–225.
21. Nissen,P., Kjeldgaard,M., Thirup,S., Polekhina,G., Reshetnikova,L., Clark,B. and Nyborg,J. (1995) Crystal structure of the ternary complex of Phe-tRNA^{Phe}, EF-Tu, and a GTP analog. *Science*, **270**, 1464–1472.
22. Nissen,P., Thirup,S., Kjeldgaard,M. and Nyborg,J. (1999) The crystal structure of Cys-tRNA^{Cys}-EF-Tu-GDPNP reveals general and specific features in the ternary complex and in tRNA. *Structure*, **7**, 143–156.
23. Ohtsuki,T., Watanabe,Y., Takemoto,C., Kawai,G., Ueda,T., Kita,K., Kojima,S., Kaziro,Y., Nyborg,J. and Watanabe,K. (2001) An 'elongated' translation elongation factor Tu for truncated tRNAs in nematode mitochondria. *J. Biol. Chem.*, **276**, 21571–21577.
24. Ohtsuki,T., Sato,A., Watanabe,Y. and Watanabe,K. (2002) A unique serine-specific elongation factor Tu found in nematode mitochondria. *Nature Struct. Biol.*, **9**, 669–673.
25. Lavrov,D.V. and Brown,W.M. (2001) *Trichinella spiralis* mt DNA: a nematode mitochondrial genome that encodes a putative ATP8 and normally structured tRNAs and has a gene arrangement relatable to those of coelomate metazoans. *Genetics*, **157**, 621–637.
26. Inaba,T., Sato,H. and Kamiya,H. (2003) Monoclonal IgA antibody-mediated expulsion of Trichinella from the intestine of mice. *Parasitology*, 591–598.
27. Thompson,J.D., Higgins,D.G. and Gibson,T.J. (1994) CLUSTAL W: improving the sensitivity of progressive multiple sequence alignment through sequence weighting, position-specific gap penalties and weight matrix choice. *Nucleic Acids Res.*, **22**, 4673–4680.
28. Guindon,S. and Gascuel,O. (2003) A simple, fast, and accurate algorithm to estimate large phylogenies by maximum likelihood. *Syst. Biol.*, **52**, 696–704.
29. Whelan,S. and Goldman,N. (2001) A general empirical model of protein evolution derived from multiple protein families using a maximum-likelihood approach. *Mol. Biol. Evol.*, **18**, 691–699.
30. Ota,T. and Nei,M. (1994) Estimation of the number of amino-acid substitutions per site when the substitution rate varies among sites. *J. Mol. Evol.*, **38**, 642–643.
31. Sakurai,M., Ohtsuki,T. and Watanabe,K. (2005) Modification at position 9 with 1-methyladenosine is crucial for structure and function of nematode mitochondrial tRNAs lacking the entire T-arm. *Nucleic Acids Res.*, **33**, 1653–1661.
32. Fechter,P., Rudinger,J., Giege,R. and Theobald-Dietrich,A. (1998) Ribozyme processed tRNA transcripts with unfriendly internal promoter for T7 RNA polymerase: production and activity. *FEBS Lett.*, **436**, 99–103.
33. Shimada,N., Suzuki,T. and Watanabe,K. (2001) Dual mode recognition of two isoacceptor tRNAs by mammalian mitochondrial seryl-tRNA synthetase. *J. Biol. Chem.*, **276**, 46770–46778.
34. Hohsaka,T., Ashizuka,Y., Murakami,H. and Sisido,M. (1996) Incorporation of nonnatural amino acids into streptavidin through *in vitro* frame-shift suppression. *J. Am. Chem. Soc.*, **118**, 9778–9779.
35. Heckler,T.G., Chang,L.H., Zama,Y., Naka,T., Chorghade,M.S. and Hecht,S.M. (1984) T4 RNA ligase mediated preparation of novel 'chemically misacylated' tRNA^{Phe}s. *Biochemistry*, **23**, 1468–1473.
36. Pingoud,A., Urbanke,C., Krauss,G., Peters,F. and Maass,G. (1977) Ternary complex formation between elongation factor Tu, GTP and aminoacyl-tRNA: an equilibrium Study. *Eur. J. Biochem.*, **78**, 403–409.
37. Lavrov,D.V. and Brown,W.M. (2001) *Trichinella spiralis* mtDNA: a nematode mitochondrial genome that encodes a putative ATP8 and normally structured tRNAs and has a gene arrangement relatable to those of coelomate metazoans. *Genetics*, **157**, 621–637.
38. LaRiviere,F.J., Wolfson,A.D. and Uhlenbeck,O.C. (2001) Uniform binding of aminoacyl-tRNAs to elongation factor Tu by thermodynamic compensation. *Science*, **294**, 165–168.
39. Gebhardt-Singh,E. and Sprinzl,M. (1986) Ser-tRNAs from bovine mitochondrion form ternary complexes with bacterial elongation factor Tu and GTP. *Nucleic Acids Res.*, **14**, 7175–7188.
40. Wakita,K., Watanabe,Y., Yokogawa,T., Kumazawa,Y., Nakamura,S., Ueda,T., Watanabe,K. and Nishikawa,K. (1994) Higher-order structure of bovine mitochondrial tRNA^{Phe} lacking the 'conserved' GG and T psi CG sequences as inferred by enzymatic and chemical probing. *Nucleic Acids Res.*, **22**, 347–353.
41. Woriax,V.L., Burkhart,W. and Spremulli,L.L. (1995) Cloning, sequence analysis and expression of mammalian mitochondrial protein synthesis elongation factor Tu. *Biochim. Biophys. Acta*, **1264**, 347–356.
42. Andersen,G.R., Thirup,S., Spremulli,L.L. and Nyborg,J. (2000) High resolution crystal structure of bovine mitochondrial EF-Tu in complex with GDP. *J. Mol. Biol.*, **297**, 421–436.
43. Lewis,D.L., Farr,C.L. and Kaguni,L.S. (1995) *Drosophila melanogaster* mitochondrial DNA: completion of the nucleotide sequence and evolutionary comparisons. *Insect. Mol. Biol.*, **4**, 263–278.

Contribution of IL-18 to atopic-dermatitis-like skin inflammation induced by *Staphylococcus aureus* product in mice

Makoto Terada*†, Hiroko Tsutsui†‡§, Yasutomo Imai†¶, Koubun Yasuda†‡, Hitoshi Mizutani†¶, Kiyofumi Yamanishi‡‖, Masato Kubo**, Kiyoshi Matsui*, Hajime Sano*, and Kenji Nakanishi†‡††

*Division of Rheumatology and Clinical Immunology, Department of Internal Medicine, and Departments of †Immunology and Medical Zoology and ‖Dermatology, Hyogo College of Medicine, Nishinomiya 663-8501, Japan; ‡Core Research for Evolutional Science and Technology (CREST), Japan Science and Technology Agency, Kawaguchi 332-0012, Japan; ¶Department of Dermatology, Mie University School of Medicine, Tsu 514-8507, Japan; and **Laboratory for Signal Network, RIKEN Research Center for Allergy and Immunology, RIKEN Yokohama Institute, Yokohama, Kanagawa 230-0045, Japan

Communicated by Tadamitsu Kishimoto, Osaka University, Osaka, Japan, April 10, 2006 (received for review November 30, 2005)

Atopic dermatitis (AD) is a common inflammatory skin disease of unknown etiology. Cutaneous infection with microbes such as *Staphylococcus aureus* and/or skin cleansing with detergent exacerbates clinical AD. Here, we generated an AD animal model by destroying skin barrier function with detergent and subsequent topical application of protein A from *S. aureus* (SpA). NC/Nga mice, which genetically have reduced skin barrier function, and BALB/c mice having intact skin barrier function, were susceptible to this combination and developed severe and moderate AD, respectively, associated with dermal accumulation of eosinophils and mast cells. Both types of mice showed an increase in serum levels of IL-18, but not IgE. The epidermis of the NC/Nga mice rapidly expressed T helper type 1 (Th1)-associated chemokines, including ligands for CXCR3 and CCR5, after application of both SpA and detergent, but not after application of detergent alone. Although treatment with detergent induced moderate Th1 cell response, additional SpA treatment was a prerequisite for induction of the differentiation of naive T cells toward unique Th1 cells, termed "super Th1 cells," capable of producing both Th1 (IFN-γ) and T helper type 2 cytokine (IL-13), as well as IL-3, and expressing CXCR3 and CCR5. Induction of super Th1 cells required IL-18 stimulation. Blockade of IL-18 prevented AD development, whereas blockade of IL-3 partially prevented AD development, suggesting a contribution of IL-18-dependent IL-3 production to AD with cutaneous mastocytosis. *il18*$^{-/-}$BALB/c mice similarly evaded SDS/SpA-induced AD. Thus, IL-18 might be important for the development of infection-associated AD by induction of IL-3 from super Th1 cells.

IL-3 | protein A | IFN-γ | super Th1 cells | intrinsic atopic dermatitis

Atopic dermatitis (AD) is a common inflammatory skin disease. Major features of AD are pruritus, chronic relapsing course, and genetic predisposition (1–3). AD is divided into two types: (*i*) AD associated with IgE-mediated responses, affecting 70–80% of patients and termed "extrinsic AD," and (*ii*) AD without IgE-mediated responses, affecting 20–30% of patients and termed "intrinsic AD." Patients with extrinsic AD show preferential deviation toward T helper type 2 (Th2) responses, together with accumulation of Th2 chemokines such as CCL17 (thymus- and activation-regulated chemokine) and CCL22 (monocyte-derived chemokine) in the cutaneous lesions (1, 2). However, recent clinical studies have revealed that the immunological aspects of the skin lesions are quite different among the clinical stages of AD (1–3). Nonetheless, the immunopathological bases for intrinsic AD are still unknown.

Recently, we showed that transgenic mice that oversecrete IL-18 from their epidermal cells spontaneously develop AD-like dermatitis under specific pathogen-free (SPF) conditions, and that the deletion of *il18*, but not *stat6*, which encodes a signaling molecule necessary for Th2 and IgE responses, protects against the development of AD (4, 5). This finding suggests that excessive cutaneous IL-18 release is a causative factor for intrinsic-type AD. Recent clinical studies have revealed that IL-18 production levels closely parallel disease severity (6–8). Therefore, it is important to clarify whether, and how, endogenous IL-18 contributes to the development of AD when skin is exposed to natural infectious agents.

Although it is well documented that cutaneous infection with *Staphylococcus aureus* exacerbates clinical AD (1, 3), the underlying mechanism is not fully understood. Recently, we demonstrated that protein A (SpA), a surface molecule and virulent factor of *S. aureus* (9), stimulates mouse epidermal cells to secrete IL-18 (10). However, cutaneous application of SpA alone did not induce major skin alterations in C57BL/6 mice, despite the fact that it produced elevated serum levels of IL-18 and IgE (5, 10). This outcome led us to assume that additional factors are required for the development of AD. Because skin cleansing with detergent aggravates clinical AD (1, 11), skin barrier destruction seems to be a second important factor in AD development. Inasmuch as NC/Nga mice, which have a genetically impaired skin barrier due to reduced ceramide production (12), frequently develop AD-like dermatitis after exposure to mites (13–15), we assumed that genetic skin barrier dysfunction was a third prerequisite for the development of AD. Here, we generated an intrinsic AD mouse model by daily application of SpA, after destruction of the skin barrier with a subclinical dose of SDS, a detergent (16). Neutralizing anti-IL-18 Abs could completely protect against SDS/SpA-induced AD. Furthermore, *il18*$^{-/-}$ BALB/c mice evaded development of AD under SDS/SpA challenge. Our present results clearly demonstrate the importance of both detergent and SpA for the development of AD and provide insight into the immunopathological bases for AD. These findings also point to a possible therapeutic regimen for intrinsic AD that would target IL-18.

Results

SpA-Induced AD-Like Dermatitis. Daily application of SpA after treatment with a subclinical dose of SDS dose-dependently induced AD-like dermatitis in NC/Nga mice under SPF conditions (Figs. 1*A* and 2*A*). However, application of SpA without prior SDS treatment did not induce any skin alterations (Figs. 1*A* and 2*A*), indicating a requirement for both SpA and SDS. Because 4% SDS and 200 μg of SpA induced the highest levels of skin alteration in all NC/Nga

Conflict of interest statement: No conflicts declared.

Abbreviations: AD, atopic dermatitis; Th2, T helper type 2; SPF, specific pathogen-free; SpA, *Staphylococcus aureus* protein A; Th1, T helper type 1; LN, lymph node.

§Present addresses: Department of Microbiology, Hyogo College of Medicine, Nishinomiya 663-8501, Japan; and Core Research for Evolutional Science and Technology (CREST), Japan Science and Technology Agency, Kawaguchi 332-0012, Japan.

††To whom correspondence should be addressed at: Department of Immunology and Medical Zoology, Hyogo College of Medicine, 1-1, Mukogawa-cho, Nishinomiya, 663-8501 Japan. E-mail: nakaken@hyo-med.ac.jp.

www.pnas.org/cgi/doi/10.1073/pnas.0602900103

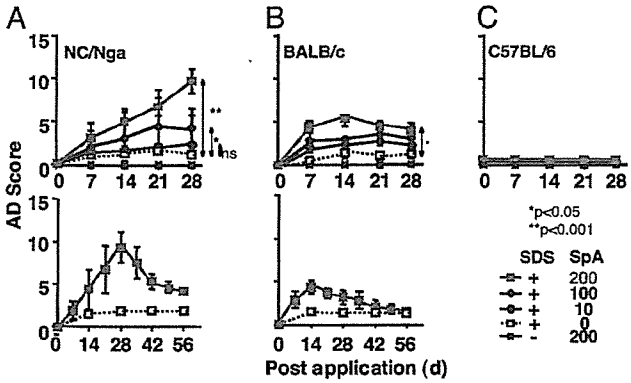

Fig. 1. Comparison of susceptibility to SDS/SpA-induced AD. NC/Nga (*A*), BALB/c (*B*), and C57BL/6 (*C*) mice were treated daily with (+) or without (−) 4% SDS and subsequently with various doses (μg) of SpA for the indicated days after challenge. AD scores were determined as described in ref. 13. ns, not significant. *A* and *B Lower* show some of the same data on a longer time scale.

mice, we used this combination in our study. The AD score (13) peaked at 4 weeks and then declined gradually, but still to a level higher than basal level (Fig. 1*A*). Thus, NC/Nga mice are highly susceptible to the combined application of SDS and SpA. BALB/c mice, although they evaded spontaneous skin alterations under conventional conditions, exhibited dermatitis phenotypically similar to that in NC/Nga mice, but with much lower AD scores (Fig. 1*B*). In BALB/c mice, the AD score peaked at 2 weeks after application and then declined to the lowest levels equivalent to those in mice treated with SDS alone (Fig. 1*B*). Thus, BALB/c mice are moderately susceptible to combined application of SDS and SpA, whereas C57BL/6 mice are resistant (Fig. 1*C*). Because NC/Nga mice developed severe and persistent AD-like clinical AD, we used this strain of mouse in our analysis. Sequential treatment with SDS and BSA or ovalbumin instead of SpA did not induce skin alterations in NC/Nga mice (data not shown), suggesting that SpA does not simply serve as a foreign antigen (Ag). Thus, we found that SDS/SpA-induced AD depended on genetic predisposition, including skin barrier dysfunction (12).

Inflammatory Skin Alterations with Mast Cell Accumulation. Histological analyses revealed epidermal hyperplasia (acanthosis) and inflammatory changes in the dermis of the skin sites of SDS/SpA-treated mice (Fig. 2*B*). The dermis was densely infiltrated with various subtypes of leukocytes, including eosinophils and mast cells (Fig. 2*B*). Focal accumulations of eosinophils were observed in the s.c. layer (Fig. 2*B Inset*). In contrast, mice treated with SDS alone showed only minor skin alteration (Fig. 2*B*).

The skin sites showed increased T cell numbers and MHC class II levels (Fig. 2*B*), suggesting cutaneous accumulation of IFN-γ (17). However, mice treated with SDS alone had nearly intact skin (Fig. 2*B*).

Plasma histamine levels closely paralleled the degree of mastocytosis observed (Fig. 2 *C* and *D*), indicating the presence of activated mast cells. However, serum levels of IgE were not elevated (Fig. 2*E*). Collectively, these results indicated that SDS/SpA-induced dermatitis is a good intrinsic animal model for AD and suggested that IgE is not principally involved in the development of this dermatitis.

Differentiation Toward Super T Helper Type 1 (Th1) Cells Producing Th1 Cytokine, IL-3, and IL-13, but Not IL-4. To address the mechanism underlying the up-regulated MHC class II expression, we investigated whether CD4$^+$ T cells differentiated toward Th1 cells. CD4$^+$ T cells from the regional lymph nodes (LNs) of treated mice at days

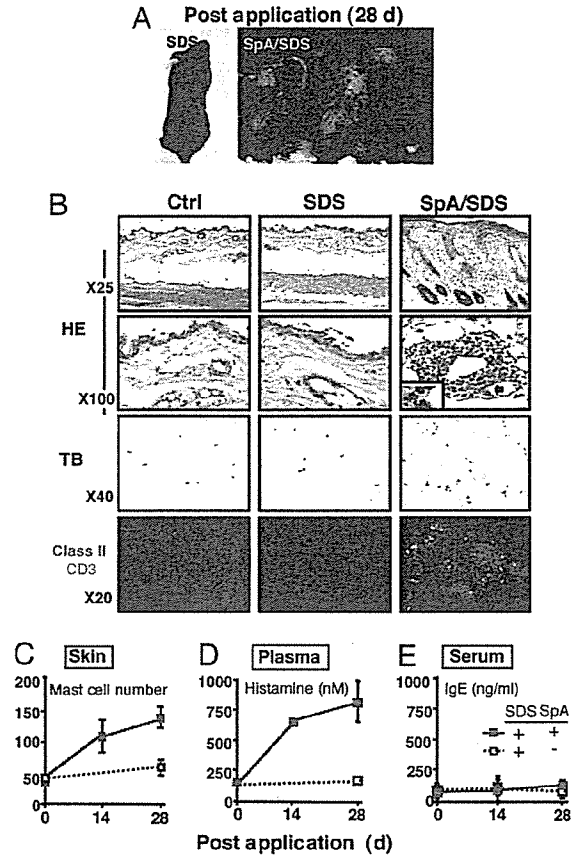

Fig. 2. SDS/SpA-induced AD. NC/Nga mice were treated daily with 4% SDS and subsequently with 200 μg SpA. (*A*) Representative photographs at day 28. (*B*) Cutaneous sections prepared from mice treated with SpA and/or SDS for 28 days or from untreated mice (Ctrl) were stained with hematoxylin and eosin (HE) or toluidine blue (TB). The arrow denotes eosinophils, magnified in *Inset*. Frozen skin sections were incubated with phycoerythrin-conjugated MHC class II and FITC-conjugated anti-CD3. (*C*) Mast cells were counted in the skin sections. (*D* and *E*) Plasma and serum were sampled, and histamine (*D*) and IgE (*E*) were measured by ELISA.

1 and 2 produced larger amounts of IFN-γ than did those from untreated mice (Fig. 3*A*). The cells produced basal levels of IL-4 and IL-13, indicating rapid differentiation toward Th1 cells. Intriguingly, CD4$^+$ T cells from mice treated for 7 days and longer gained the capacity to produce much larger amounts of IL-13 and IL-3 as well (Fig. 3*A*), indicating that the CD4$^+$ T cells further differentiate into the unique cells that can produce IFN-γ, IL-3, and IL-13, but not IL-4. We propose to designate this subpopulation as "super Th1 cells" with regard to their unique potential to produce both Th1- and Th2-related proinflammatory cytokines, each of which is involved in various inflammatory tissue diseases (17–20). In contrast, CD4$^+$ LN cells from SDS-treated mice showed a simple and moderate shift to Th1 cells (Fig. 3*A*), as was also the case for CD4$^+$ LN cells from ovalbumin/SDS-treated mice that had no apparent dermatitis (data not shown). These results clearly indicate that the regional LN cells develop toward super Th1 cells after SDS/SpA application and suggest that the Th1-driving condition attainable with SDS treatment was insufficient for the development of AD.

Next, we investigated whether IL-12 and IL-18, prototype cytokines for Th1 cell development (21), are accumulated in treated mice. Regional LNs expressed *il12* after SDS/SpA challenge (Fig. 3*B*). Intriguingly, SDS by itself can induce *il12* expression (Fig. 3*B*),

IMMUNOLOGY

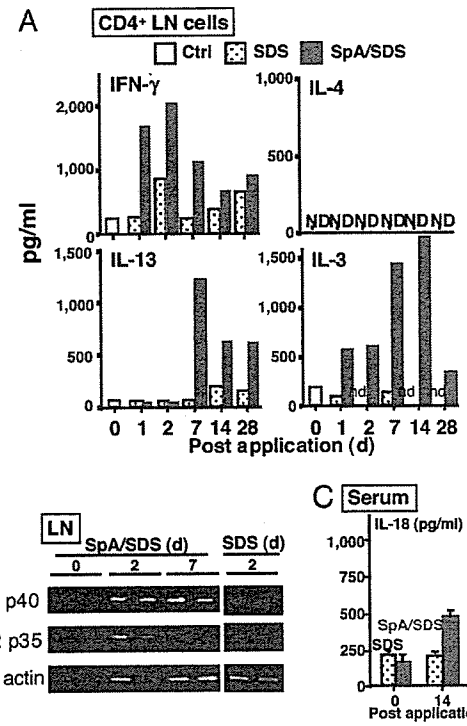

Fig. 3. Differentiation of regional LN CD4+ cells into super Th1 cells. NC/Nga mice were treated daily with SDS or SDS/SpA. CD4+ cells were isolated from the cervical and axillary LNs, pooled, and incubated with immobilized anti-CD3 for 48 hr. Concentrations of IFN-γ, IL-3, IL-4, and IL-13 were determined by ELISA (*A*). The cervical and axillary LNs (*B*) and sera (*C*) were sampled, and expressions of *il12 p40* and *il12 p35* (*B*) and IL-18 levels (*C*) were determined by RT-PCR and ELISA, respectively. Photographs are representative of three independent experiments with similar results. ND, not detected; nd, not done.

indicating the importance of SDS for IL-12 production. Consistent with our previous report (10), in NC/Nga (Fig. 3*C*), BALB/c, and C57BL/6 mice (data not shown), IL-18 accumulated in the circulation after application of SDS/SpA but not SDS alone.

Requirement of IL-18 for Super Th1 Cell Development. Our observations led us to assume that IL-18, together with IL-12, commits naive CD4+ T cells to the formation of super Th1 cells. To evaluate this assumption, we incubated naive NC/Nga CD4+ LN cells under Th1 condition supplemented with IL-18 (Th1 + IL-18), as described in *Methods*, and examined the cells' production of IFN-γ, IL-3, and IL-13 upon stimulation with anti-CD3. The CD4+ T cells primed under Th1 + IL-18 produced all of the cytokines except IL-4 (Fig. 4*A*), demonstrating and mimicking the potential for IL-18 to supershift toward super Th1 cells *in vivo*. Notably, super Th1 cells produced larger amounts of IL-3 and IL-13, but still no IL-4, after challenge with immobilized anti-CD3 + IL-18 (Fig. 4*A*). Consistent with our previous report (22), 8.5% of CD4+ T cells primed under Th1 + IL-18, but none of those primed under simple Th1 condition, expressed both Th1 cytokines (e.g., IFN-γ) and Th2 cytokines (e.g., IL-13) by cytoplasmic cytokine staining (data not shown). In a separate experiment, we observed that IFN-γ+ cells purified from super Th1 cells by capturing secreted IFN-γ (22) produce IL-3 and IL-13 in response to immobilized anti-CD3 + IL-18 (data not shown). Thus, anti-CD3 stimulation synergizes with IL-18 to produce IL-3 and IL-13 selectively from super Th1 cells. BALB/c CD4+ LN cells differentiated into super Th1 cells when primed under Th1 + IL-18, confirming this as a super Th1 cell-inducing

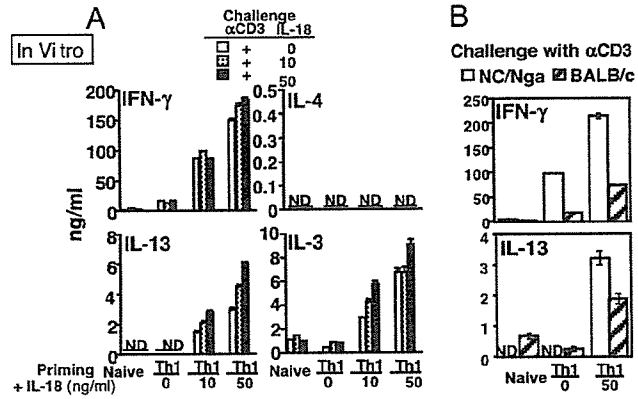

Fig. 4. Requirement of IL-12 and IL-18 for super Th1 cell development. CD4+ LN cells from naive NC/Nga (*A* and *B*) or BALB/c (*B*) mice were stimulated with various doses of IL-18 under Th1 cell conditions. The cells were freshly challenged with immobilized anti-CD3 with (*A*) or without (*B*) various doses of IL-18 for 48 hr, and cytokine concentrations were measured. ND, not detected.

condition (Fig. 4*B*). All of these results indicate that IL-18 is an inducer and activator of super Th1 cells.

Rapid Induction of IFN-γ, IL-13, IL-3, and Th1 Chemokines in the Skin Sites of Treated Mice. It is important to note that the treated skin sites quickly began to express the super Th1-associated cytokines and chemokines required for the recruitment of super Th1 cells (23, 24). We measured levels of these cytokines in the skin site homogenates. Concentrations of IFN-γ, IL-13, and IL-3, but not IL-4, were increased (Fig. 5*A*), indicating that the super Th1 cells are recruited and produce these cytokines *in vivo*.

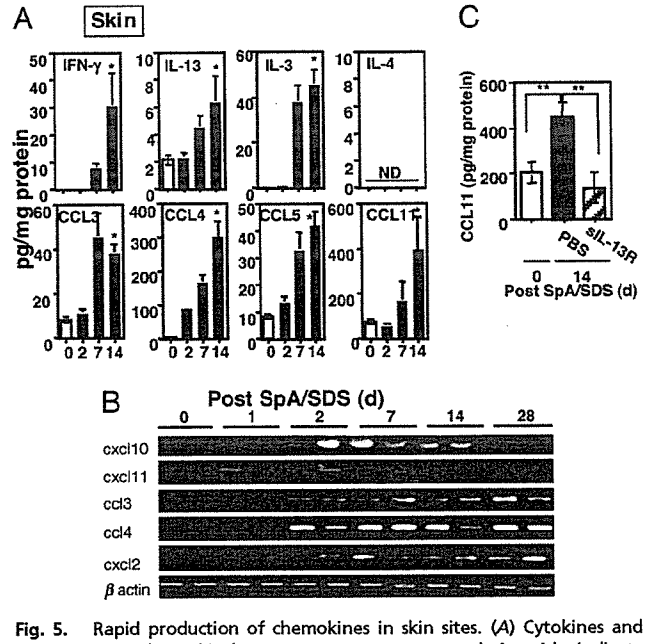

Fig. 5. Rapid production of chemokines in skin sites. (*A*) Cytokines and chemokine levels in skin homogenates were measured. Asterisks indicate significant increase ($P < 0.05$) of the individual molecules as compared with those at day 0. (*B*) Total RNA was extracted from the skin specimens and RT-PCR was performed. Photographs are representative of three independent experiments with similar results. (*C*) Mice were treated with or without SDS/SpA (open bar) and additionally treated with soluble IL-13Rα2-Fc (sIL-13R, hatched bar) or vehicle (PBS, filled bar). CCL11 concentrations in the skin homogenates at day 14 were measured. **, $P < 0.01$.

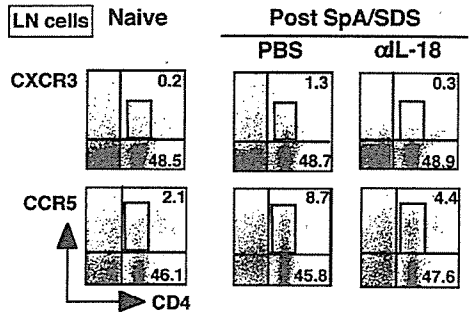

Fig. 6. IL-18-dependent CXCR3 and CCR5 expression on $CD4^+$ LN cells. LN cells were prepared from naive mice or from PBS- or anti-IL-18-treated SDS/SpA-challenged mice at day 2 or day 7 and examined for their expression of CD4/CXCR3 and CD4/CCR5 by FACS. Numbers in the upper right corner of each graph indicate the percentage of cells expressing both CD4 and corresponding chemokine receptor gated in a square. Numbers in the lower right corner indicate the percentage of $CD4^+$ cells negative for these receptors.

SDS/SpA application simultaneously induced rapid production of CCL3 [macrophage inflammatory protein (MIP)-1α], CCL4 (MIP-1β), CCL5 [regulated on activation normal T cell expressed and secreted (RANTES)], and CCL11 (eotaxin) (Fig. 5 *A* and *B*), which can recruit various subtypes of leukocytes, including mast cells and eosinophils. This change was also the case for *cxcl 10* (*ip10*), *cxcl 11* (*i-tac*), and *cxcl2*, which can recruit macrophages, T cells, and neutrophils (Fig. 5*B*). However, treatment with SDS alone did not induce these chemokine messages (data not shown). These results indicated the importance of SpA for induction of the expression of chemokines.

Because IL-13 is a potent stimulus for CCL11 production (25), we investigated possible involvement of IL-13 in the elevated CCL11 expression. Treatment with IL-13 antagonist inhibited the elevation of cutaneous CCL11 (Fig. 5*C*), indicating that IL-13 is required for the production of CCL11.

IL-18 Induction of Chemokine Receptor Expressions on Super Th1 Cells. Next, we investigated the mechanism underlying the recruitment of super Th1 cells into the skin sites. Because CXCR3 and CCR5 recognize CXCL10/CXCL11 and CCL3/CCL4/CCL5, respectively, we analyzed CXCR3 and CCR5 expression on the regional LN $CD4^+$ cells. Both CXCR3 and CCR5 expressions were induced on the LN $CD4^+$ cells after SDS/SpA application (Fig. 6).

We then examined the possible involvement of IL-18 in these chemokine receptor inductions. IL-18 blockade prevented induction of CXCR3 and CCR5 (Fig. 6), indicating the requirement of IL-18 for CXCR3 and CCR5 inductions on super Th1 cells.

Contribution of Endogenous IL-18 to the Development of AD. We tested whether endogenous IL-18 is required for the development of SDS/SpA-induced AD. Mice treated with neutralizing anti-IL-18 had profoundly reduced AD scores, with little epidermal hyperplasia; little infiltration with T cells, eosinophils, and neutrophils; and basal levels of mast cells and MHC class II (Fig. 7 *A* and *B*). To formally establish the essential role of endogenous IL-18, we applied SDS/SpA to *il18*$^{-/-}$ BALB/c mice. Wild-type BALB/c mice exhibited AD-associated histological changes resembling those in NC/Nga mice, whereas *il18*$^{-/-}$ BALB/c mice were nearly free from these changes (Fig. 7*C*), again pointing to IL-18 as a causative factor. These results indicated that endogenous IL-18 is essential for the development of SDS/SpA-induced AD.

Involvement of IL-3 in the Induction of Cutaneous Mastocytosis. Because differentiation toward Th1 cells precedes differentiation toward super Th1 cells (Fig. 3*A*) and fundamentally requires IFN-γ

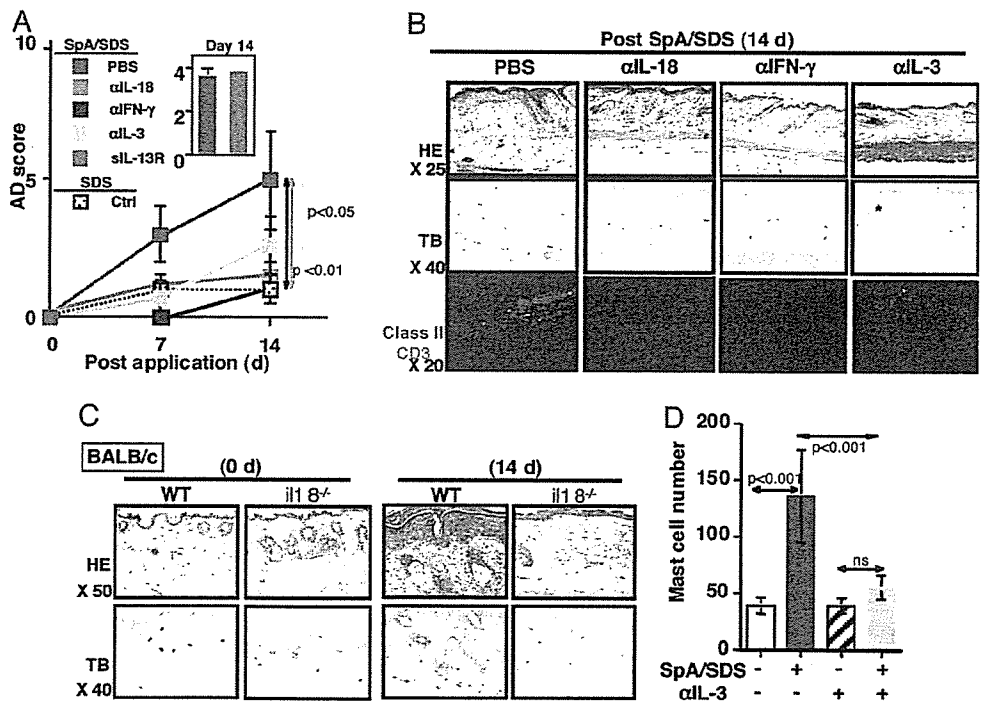

Fig. 7. IL-18 as a potent therapeutic target for SDS/SpA-induced AD. (*A*, *B*, *D*) NC/Nga mice were administered PBS, anti-IL-18 Abs (αIL-18), anti-IFN-γ Abs (αIFN-γ), or anti-IL-3 Abs (αIL-3) i.p. during SDS/SpA challenge. For control study, NC/Nga mice were treated with SDS alone. (*A Inset*) NC/Nga mice were administered PBS (red bar) or soluble IL-13Rα2-Fc (sIL-13R, gray bar) i.p. (*A*) AD sores were determined. (*B*) Histological and immunohistological analyses were performed. Asterisks indicate the sites with epidermal hyperplasia of anti-IL-3-treated, SDS/SpA-challenged mice. (*C*) Wild-type or *il18*$^{-/-}$ BALB/c mice were examined on day 0 (*Left*) or were treated daily with SDS/SpA for 14 days (*Right*). (*D*) Mast cell numbers were counted. ns, not significant.

(17), we investigated the role of IFN-γ. Treatment with neutralizing anti-IFN-γ protected against the development of AD concomitant with inhibition of elevated MHC class II expression (Fig. 7 *A* and *B*), indicating the requirement of IFN-γ for AD development. To investigate how super Th1 cells are involved, we examined the roles of cytokines produced by the super Th1 cells but poorly by Th1 cells. Although treatment with IL-13 antagonist profoundly inhibited the elevation of CCL11 (Fig. 5*C*), this treatment did not reduce the AD scores until day 14 (Fig. 7*A Inset*), indicating a minor role for IL-13. Because IL-3 induces mast cell proliferation/activation (20) synergistically with IL-18 (26), we investigated the possible involvement of IL-3. Blockade of IL-13 profoundly inhibited mastocytosis (Fig. 7*D*) and substantially protected against AD development (Fig. 7 *A* and *B*). On the basis of all our observations, we conclude that super Th1 cells contribute to the development of AD at least partly by producing IL-3 in response to IL-18.

Discussion

We generated an intrinsic AD mouse model by the application of detergent and subsequently SpA. SDS treatment induced the expression of IL-12, and possibly other cytokines such as IL-23. Topical application of SpA induces the release of IL-18 from keratinocytes. We have provided evidence that IL-18 contributes to intrinsic AD development by inducing and activating super Th1 cells that have the potential to produce IFN-γ, IL-13, and IL-3.

Th1 responses negatively regulate Th2 responses, and vice versa. Theoretically, AD might be classified into two types: Th1 and Th2. However, individual AD patients often have mixed-type immunity (3). As in clinical AD, NC/Nga mice can develop Th1, Th2, or mixed-type AD. The mice develop Th2-type AD when kept under conventional conditions (13, 14); however, they show mixed-type AD after application of SDS/SpA under SPF conditions. In the strict sense, our SDS/SpA-induced AD model can be classified as a super Th1 type (Figs. 3*A* and 4). Therefore, it is intriguing to note that this super Th1 cell subset alone may explain the complicated immunopathology of some types of clinical AD.

Coproduction of IL-13 and IFN-γ is a hallmark for certain types of clinical AD. Indeed, lymphocytes from intrinsic AD patients produce greater amounts of IFN-γ and IL-13 than those from healthy individuals (27). There are two possible explanations for this outcome. One is that these patients have both Th1 and Th2 cells. Alternatively, the patients may have super Th1 cells. It is quite important to distinguish the latter from the former. Our present results suggest that susceptibility to intrinsic AD is at least partly determined by the intrinsic nature of T lymphocytes to preferentially develop into super Th1 cells. In fact, highly susceptible (NC/Nga) and moderately susceptible (BALB/c) mice showed robust and moderate differentiation toward super Th1 cells, respectively (Fig. 4*B*), whereas resistant C57BL/6 mice failed to develop super Th1 cells (data not shown). Notably, in both highly and moderately susceptible strains, IL-18 is commonly essential for the development of AD (Fig. 7). For patients who have predominantly super Th1 cells, a treatment targeting IL-18 might be very beneficial.

The results of our present study provide evidence that a Th1-skewing milieu can induce allergic inflammatory diseases by differentiating naive $CD4^+$ T cells into super Th1 cells, in collaboration with IL-18. Although they are a major effector cell population involved in IgE-mediated allergic inflammatory diseases, mast cells can be activated by IL-3 and IL-18 in the absence of crosslinkage of their FcεRI (20, 28–30). Super Th1 cells can be involved in dermal mastocytosis through production of IL-3 in response to Ag and IL-18 (Figs. 3*A*, 4, 5*A*, and 7). Thus, it might be IL-3 that links the Th1-driving circumstances to mast cell involvement in allergic inflammatory diseases.

Super Th1 cells characteristically produce IL-13, a central effector cytokine for the development of inflammatory tissue diseases such as bronchial asthma (18, 31–33). However, IL-13 is not intensely involved in the development of SDS/SpA-induced AD, at least in its acute phase (Fig. 7*A*). IL-13 is a potent stimulator and activator of transforming growth factor β1, a fibrogenic cytokine (31). Therefore, it is plausible that IL-13 produced by super Th1 cells is involved in the late-occurring dermal fibrosis of SDS/SpA-induced AD.

SDS/SpA-treated mice showed major clinical features of AD, indicating the suitability of SDS/SpA-induced dermatitis as an AD model. Furthermore, skin lesions of SDS/SpA-treated mice closely resemble those of clinical AD in terms of dense infiltration of eosinophils and mast cells (3, 34) and elevated histamine levels (35). SDS/SpA-treated mice showed little increase in serum IgE (Fig. 1*E*), suggesting that our model characterizes an intrinsic AD. Although it is important to know that dermal mastocytosis and elevated histamine levels, both of which are major features of this model, are more prominent in clinical intrinsic AD when compared with extrinsic AD, no appropriate clinical reports properly address this issue. Further clinical studies are needed to determine whether this model represents an intrinsic AD in the strict sense.

Notably, SpA cannot be replaced by conventional protein Ags (data not shown), suggesting that SpA might perform several functions that ovalbumin or BSA cannot. First, SpA can stimulate keratinocytes to release IL-18 (10). Second, SpA seems to directly cause rapid expression of chemokines in the skin sites (Fig. 5), as it does in the respiratory tract (9). Thus, SpA can function as a professional AD-inducing protein in certain situations, which presents the possibility that molecules that can induce IL-18 and chemokine release from epidermal cells might function as an intrinsic AD-inducing factor. Further study is needed to validate such conclusions.

We also observed that IL-18 blockade, or absence, inhibited SDS/SpA-induced AD. This finding suggests the importance of IL-18 as a therapeutic target molecule for certain atopic diseases.

Methods

Mice. NC/Nga, BALB/c, and C57BL/6 mice were purchased from Oriental Yeast (Osaka). *il18*$^{-/-}$ BALB/c mice have been described elsewhere (21). Five to seven female mice, 6–10 weeks of age, were used in each *in vivo* study as experimental and control groups. All mice were kept under SPF conditions and received humane care, as outlined in the *Guide for the Care and Use of Laboratory Animals* (36).

Reagents. SpA from *S. aureus* Cowan I was purchased from Calbiochem. Anti-CD28, anti-CD3, anti-CD4, and anti-MHC class II were from Pharmingen. Hybridomas producing neutralizing anti-IFN-γ mAb (R6A2) or anti-IL-4 mAb (11B11) were from American Type Culture Collection. Neutralizing polyclonal anti-IL-18 Abs were described elsewhere (22). Neutralizing polyclonal anti-IL-3 Abs, soluble IL-13Rα2-Fc chimera, rIL-12, and rIL-2 were from R & D Systems. Recombinant mouse IL-18 was from MBL (Nagoya, Japan).

Induction of AD. Mice were treated with 4% SDS in sterile distilled water on a 5-cm^2 area of their shaven backs, and 30 min later with SpA in sterile distilled water, once a day. In some experiments, mice received anti-IL-18 (500 μg), anti-IFN-γ (500 μg), soluble IL-13Rα2-Fc (100 μg), or anti-IL-3 (500 μg) on day 0 and every 5 days after challenge with SDS/SpA. We used *in vivo* a neutralizing dose of anti-IL-3 Abs or IL-13Rα2-Fc in accordance with the supplier's instructions or on the basis of our previous study (22). Serum, plasma, skin specimens, and axillary and cervical LNs were sampled. In some experiments, skin homogenates were prepared as described in ref. 10. A clinical AD score was determined as described in ref. 13.

Histological Study. Sections from skin specimens were stained as detailed in ref. 4. In some experiments, mast cell numbers in 10

Table 1. Primer sequences for cytokines and chemokines

Cytokine/ chemokine	Sense primer	Antisense primer	No. of PCR cycles
IL-12p35	AGACGTCTTTGATGATGACC	TCACTCTGTAAGGGTCTGCT	35
IL-12p40	CGTGCTCATGGCTGGTGCAAAG	GAACACATGCCCACTTGCTG	35
CXCL10	ACCATGAACCCAAGTGCTGCCGTC	GCTTCACTCCAGTTAAGGAGCCCT	35
CXCL11	TCTGCTGTCTTGGAACATGC	CGTGTGCCTCGTGATATTTG	35
CXCL2	GAAGTCATAGCCACTCTCAAGGGGC	CAACTCACCCTCTCCCCAGAAAC	35
CCL3	CCTCTGTCACCTGCTCAACA	CTGCCTCCAAGACTCTCAGG	35
CCL4	CCCACTTCCTGCTGTTTCTC	GGGAGACACGCGTCCTATAA	35
β-Actin	GATGACGATATCGCTGCGCTG	GTACGACCAGAGGCATACAGG	28

low-power fields selected randomly were counted (Figs. 2*C* and 7*D*).

Confocal Laser Microscopic Analysis. Frozen sections from freshly isolated skin specimens were fixed and incubated with FITC- and/or phycoerythrin-conjugated mAbs (×50), followed by evaluation using a laser scanning confocal microscope (model IX81; Olympus, Tokyo).

***In Vitro* Super Th1 Cell Differentiation.** Magnetic cell sorting system-enriched $CD4^+$ LN cells from untreated mice were incubated with 10 ng/ml rIL-12, 10 units/ml IL-2, and 10 μg/ml anti-IL-4 in the presence of rIL-18 in complete RPMI medium 1640 in an anti-CD3- (5 μg/ml) and anti-CD28 (1 μg/ml)-coated dish. Two-round cell culture was undertaken, and the cells collected were freshly incubated with immobilized anti-CD3 plus IL-18 for 48 hr.

Expression of CXCR3/CCR5 on $CD4^+$ LN Cells. Cervical and axillary LN cells prepared from NC/Nga mice at day 2 or 7 after application were incubated with allophycocyanin-conjugated anti-CD4 and phycoerythrin-conjugated anti-CXCR3 (Pharmingen) or with a battery of goat anti-CCR5 (Zymed) and FITC-conjugated anti-goat IgG, respectively (10).

ELISA for Cytokines, Chemokines, IgE, and Histamine. Concentrations of IL-4, IL-13, IL-3, and IFN-γ were determined with ELISA kits (Genzyme) or Mouse 23 Plex Panel (Bio-Rad). Histamine and IL-18 levels were determined with ELISA kits from Immunotech (Marseille, France) and MBL, respectively. Serum IgE was measured as described in ref. 4.

RT-PCR. Total RNA was extracted, and RT-PCR was performed (10). Primers for cytokines and chemokines, and the number of PCR cycles, are shown in Table 1.

Statistical Analysis. Data are shown as the mean ± SD of triplicate samples. Significance of differences between the experimental and control groups was examined by the unpaired Student's *t* test. The data are representative of three independent experiments with similar results.

We thank Drs. N. Hayashi and J. Sawaki at Hyogo College of Medicine for enthusiastic discussion and Ms. S. Yumikura-Futatsugi and Ms. N. Nakano for excellent technical assistance. This work was supported in part by grants, including a Hitec Research Center Grant, from the Ministry of Education, Culture, Sports, Science, and Technology of Japan.

1. Leung, D. Y. M. & Bieber, T. (2003) *Lancet* **361,** 151–160.
2. Kupper, T. S. & Fuhlbrigge, R. C. (2004) *Nat. Rev. Immunol.* **4,** 211–222.
3. Leung, D. Y. M., Boguniewicz, M., Howell, M. D., Nomura, I. & Hamid, Q. A. (2004) *J. Clin. Invest.* **113,** 651–657.
4. Konishi, H., Tsutsui, H., Murakami, T., Yumikura-Futatsugi, S., Yamanaka, K., Tanaka, M., Iwakura, Y., Suzuki, N., Takeda, K., Akira, S., *et al.* (2002) *Proc. Natl. Acad. Sci. USA* **99,** 11340–11345.
5. Tsutsui, H., Yoshimoto, T., Hayashi, N., Mizutani, H. & Nakanishi, K. (2004) *Immunol. Rev.* **202,** 115–138.
6. Tanaka, T., Tsutsui, H., Yoshimoto, T., Kotani, M., Matsumoto, M., Fujita, A., Wang, W., Higa, S., Kishimoto, T., Nakanishi, K. & Suemura, M. (2001) *Int. Arch. Allergy Immunol.* **125,** 236–240.
7. Ohnishi, H., Kato, Z., Watanabe, M., Fukutomi, O., Inoue, R., Teramoto, T. & Kondo, N. (2003) *Allergol. Int.* **52,** 123–130.
8. Novak, N., Kruse, S., Potreck, J., Maintz, L., Jenneck, C., Weidinger, S., Fimmer, R. & Bieber, T. (2005) *J. Allergy Clin. Immunol.* **115,** 828–833.
9. Gómez, M., Lee, A., Reddy, B., Muir, A., Soong, G., Pitt, A., Cheung, A. & Prince, A. (2004) *Nat. Med.* **10,** 842–848.
10. Nakano, H., Tsutsui, H., Terada, M., Yasuda, K., Matsui, K., Yumikura-Futatsugi, S., Yamanaka, K., Mizutani, H., Yamamura, T. & Nakanishi, K. (2003) *Int. Immunol.* **15,** 611–621.
11. Kiriyama, T., Sugiura, H. & Uehara, M. (2003) *J. Dermatol.* **30,** 708–712.
12. Aioi, A., Tonogaito, H., Suto, H., Hamada, K., Ra, C., Owaga, H., Maibach, H. & Matsuda, H. (2001) *Br. J. Dermatol.* **144,** 12–18.
13. Matsuda, H., Watanabe, N., Geba, G. P., Sperl, J., Tsudzuki, M., Hiroi, J., Matsumoto, M., Ushio, H., Saito, S., Askenase, P. W. & Ra, C. (1997) *Int. Immunol.* **9,** 461–466.
14. Vestergaard, C., Yoneyama, H., Murai, M., Nakamura, K., Tamaki, K., Terashima, Y., Imai, T., Yoshie, O., Irimura, T., Mizutani, H. & Matsushima, K. (1999) *J. Clin. Invest.* **104,** 1097–1105.
15. Yagi, R., Nagai, H., Iigo, Y., Akimoto, T., Arai, T. & Kubo, M. (2002) *J. Immunol.* **168,** 2020–2027.
16. Tsai, J.-C., Shen, L.-C., Sheu, H.-M. & Lu, C.-C. (2003) *Arch. Dermatol. Res.* **295,** 169–174.
17. Boehm, U., Klamp, T., Groot, M. & Howard, J. C. (1997) *Annu. Rev. Immunol.* **15,** 749–795.
18. Wills-Karp, M., Luyimbazi, J., Xu, X., Schofield, B., Neben, Y., Karp, C. L. & Donaldson, D. D. (1998) *Science* **282,** 2258–2261.
19. Kuperman, D. A., Huang, X., Koth, L. L., Chang, G. H., Dogganov, G. M., Zhu, Z., Elias, J. A., Sheppard, D. & Erle, D. J. (2002) *Nat. Med.* **8,** 885–889.
20. Shelburne, C. P. & Ryan, J. J. (2001) *Immunol. Rev.* **179,** 80–93.
21. Takeda, K., Tsutsui, H., Yoshimoto, T., Adachi, O., Yoshida, N., Kishimoto, T., Okamura, H., Nakanishi, K. & Akira, S. (1998) *Immunity* **8,** 383–390.
22. Sugimoto, T., Ishikawa, Y., Yoshimoto, T., Hayashi, N., Fujimoto, J. & Nakanishi, K. (2004) *J. Exp. Med.* **199,** 535–545.
23. Rossi, D. & Zlotnik, A. (2000) *Annu. Rev. Immunol.* **18,** 212–242.
24. Rot, A. & von Andrian, U. H. (2004) *Annu. Rev. Immunol.* **22,** 891–928.
25. Zhu, Z., Homer, R. J., Wang, Z., Chen, Q., Geba, G. P., Wang, J., Zhang, Y. & Elias, J. A. (1999) *J. Clin. Invest.* **103,** 779–788.
26. Yoshimoto, T., Tsutsui, H., Tominaga, K., Hoshino, K., Okamura, H., Akira, S., Paul, W. E. & Nakanishi, K. (1999) *Proc. Natl. Acad. Sci. USA* **96,** 13962–13966.
27. Simon, D., Borelli, S., Braathen, L. & Simon, H. (2002) *Allergy* **57,** 431–435.
28. Hamaguchi, Y., Kanakura, Y., Fujita, J., Takeda, S., Nakano, T., Tarui, S., Honjo, T. & Kitamura, Y. (1987) *J. Exp. Med.* **165,** 268–273.
29. Matsuura, N. & Zetter, B. R. (1989) *J. Exp. Med.* **170,** 1421–1426.
30. Galli, S. J., Kalensnikoff, J., Grimbaldeston, M. A., Piliponsky, A. M., Williams, C. M. M. & Tsai, M. (2005) *Annu. Rev. Immunol.* **23,** 749–786.
31. Wynn, T. A. (2003) *Annu. Rev. Immunol.* **21,** 425–456.
32. Ford, J. G., Rennick, D., Donaldson, D. D., Venkayya, R., McArthur, C., Hansell, E., Kurup, V. P., Warnock, M. & Grünig, G. (2001) *J. Immunol.* **167,** 1769–1777.
33. Wills-Karp, M. (2004) *Immunol. Rev.* **202,** 175–190.
34. Mihm, M. C., Jr., Soter, N. A., Dvorak, H. F. & Austen, K. F. (1976) *J. Invest. Dermatol.* **67,** 305–312.
35. Steinhoff, M., Neisius, U., Ikoma, A., Fartasch, M., Heyer, G., Skov, P. S., Luger, T. A. & Schmelz, M. (2003) *J. Neurosci.* **23,** 6176–6180.
36. Institute of Laboratory Animal Resources, National Research Council (1996) *Guide for the Care and Use of Laboratory Animals* (Natl. Acad. Press, Washington, DC).